



Paleomagnetic study of NeoArchean–Paleoproterozoic dykes in the Kaapvaal Craton

Natalia Lubnina^{a,*}, Richard Ernst^{b,c}, Martin Klausen^d, Ulf Söderlund^e

^a Department of Dynamic Geology, Moscow State University, Leninskiye Gory, Moscow 119992, Russia

^b Ernst Geosciences 43 Margrave Ave., Ottawa, K1T 3Y2, Canada

^c Carleton University, Ottawa, K1S 5B6, Canada

^d Department of Earth Sciences, University of Stellenbosch, Private Bag X1, Matieland 7602, South Africa

^e Lund University, Geobiosphere Science Centre, Department of Geology, Sölvegatan 12, SE 223 62 Lund, Sweden

ARTICLE INFO

Article history:

Received 5 May 2009

Received in revised form 7 March 2010

Accepted 3 May 2010

Keywords:

Paleomagnetism

NeoArchean–Paleoproterozoic

Kaapvaal Craton

U–Pb dating

Baddeleyite

ABSTRACT

431 oriented samples were collected from 27 dolerite dykes at 17 sites, belonging to 2.95, 2.65, and 1.90 Ga swarms, that trend SE, E and NE, respectively from the Bushveld Igneous Complex into the eastern Kaapvaal Craton (ages determined by Olsson et al., 2010; Olsson in Söderlund et al., this volume). Samples were analyzed for paleomagnetism and also anisotropy of magnetic susceptibility (AMS). For the 2.95 Ga SE-trending dykes high temperature/coercivity 'P' component has unblocking temperatures up to 590 °C and coercivity 40–90 mT and demonstrate SSW declination and intermediate positive inclination. Based on positive contact and conglomerate tests we argue for a primary origin of this component. The paleopole (BAD), calculated from 'P' component, does not correspond to any of the previously obtained Archean–Paleoproterozoic paleopoles for the Kaapvaal Craton, and represents a new key pole for 2.95 Ga. The high-coercivity 'H' component for the 2.65 Ga-old E-trending dykes has a SSW declination and steep positive inclination. Paleomagnetic pole (RYK), recalculated from this component, is close to the paleopoles, obtained by Wingate (1998) and Strik et al. (2007) for 2.78 Ga Ventersdorp volcanics. The third group, NE-trending dykes of the 1.90 Ga Black Hill swarm demonstrate an 'M' component with dual polarity high-coercivity component with SSE-declination and negative intermediate inclination. The paleopole (BHD), calculated from this component is close to the 1.87 Ga pole of the Kaapvaal Craton obtained by Hanson et al. (2004). Overprint directions include a very well developed thermo-chemical overprint (Dec = 329° Inc = –36°), which is believed to be associated with a ~0.18 Ga regional 'Karoo' thermal event.

© 2010 Elsevier B.V. All rights reserved.

1. Introduction

Many greenstone belts terminate at a high angle to the current margins of the Kaapvaal Craton, indicating that this craton is truncated and may have belonged to a larger supercraton that, possibly, fragmented at different stages during the Paleoproterozoic, prior to the amalgamation of the Limpopo, Kheis, Namaqua-Natal and Mozambique mobile belts (e.g., Jacobs et al., 2008). Various Neoproterozoic supercratonic arrangements have been proposed (e.g., Rogers, 1996; Aspler and Chiarenzelli, 1998), but there is no consensus regarding nearest neighbors for the Kaapvaal Craton, except for a proposed linkage ("Vaalbara") with the Pilbara craton (Cheney, 1996; Wingate, 1998; Nelson et al., 1999; Eriksson et al., 2009). Other than this link, the identification of other

blocks formerly adjacent to other sides of the Kaapvaal in the NeoArchean–Paleoproterozoic is unknown.

Nevertheless, the robust identification of former nearest neighbors to the Kaapvaal Craton in the latest Archean to early Proterozoic is of significance for allowing the correlation of geological belts and boundaries, sedimentary basins, lithospheric roots, etc., between the Kaapvaal Craton and its former neighbors. In addition, there are potential economic implications to be gained from the tracing of metallogenic provinces between blocks. For instance, the economically important ca. 2060 Ma Bushveld event consists of the well-known Bushveld Igneous Complex as well as additional smaller intrusions and extrusions which are widespread in the Kaapvaal Craton (e.g., Mapeo et al., 2006). Additional units of the Bushveld event should be present on the former nearest neighbors to the Kaapvaal Craton.

Paleomagnetism offers a robust approach for producing well-constrained reconstructions. There have been several previous paleomagnetic studies of NeoArchean and Paleoproterozoic units of the Kaapvaal (e.g., Pisarevsky, 2005). However, the general prob-

* Corresponding author. Tel.: +7 495 9392551; fax: +7 495 9392551.

E-mail address: natlubnina@yandex.ru (N. Lubnina).

lem with obtaining Precambrian paleomagnetic poles, not only in the Kaapvaal Craton, but globally, has been the absence of precise dates on the units studied paleomagnetically. This problem has been noted by Buchan et al. (2000), who surveyed the available 'key paleomagnetic' poles for Laurentia and Baltica, i.e., those for which there was a robust paleomagnetic direction that averaged secular variation, was demonstrated primary on the basis of a field test, and had also a precise age date. Of the hundreds of poles published for Precambrian units, only a handful were considered 'key poles', and of these, the majority were in the Canadian shield.

A reliable Proterozoic APWP (Apparent Polar Wander Path) for the Kaapvaal Craton does not exist. Toward this goal we initiated a paleomagnetic study of units that have been precisely dated by the U–Pb baddeleyite method in companion studies (Olsson et al., 2010; Olsson in Söderlund et al., 2010). As in these dating studies, we focus on the dyke swarms that have trends which appear to radiate from the eastern side of the Bushveld Complex. We aim to obtain new paleomagnetic results on the two swarms precisely dated in the above mentioned study by Olsson et al. (2010): a SW-trending swarm of age 2965 Ma (referred to as 2.95 Ga), an E–W trending swarm with an age range of 2685–2660 Ma (referred to as 2.65 Ga). We also present paleomagnetic results for a NE-trending dyke swarm with a preliminary age of ca. 1.90 Ga (Olsson in Söderlund et al., 2010; Klausen et al., 2010). We propose new paleomagnetic poles for the Kaapvaal Craton for these times. We also use AMS (anisotropy of magnetic susceptibility) data in order to determine magma flow direction (e.g., Ernst and Baragar, 1992; Tarling and Hrouda, 1993; Polteau et al., 2008).

2. Regional geology

We refrain from any extensive review of South Africa's Neoproterozoic to Paleoproterozoic geology and refer the reader to both Johnson et al. (2006) and regional geology sections in companion papers in this volume (Olsson et al., 2010; Klausen et al., 2010). Instead, we focus our brief summary on (1) host rock units within the studied part of the Kaapvaal Craton (Fig. 1a), (2) surrounding cover rocks that are younger than 2.7 Ga, and (3) relevant aspects of the complex array of mafic dyke swarms that cross-cut various parts of the eastern Kaapvaal Craton (Fig. 1b–e).

2.1. Eastern Kaapvaal Craton basement and Pongola Supergroup

Fig. 1(a) shows the distribution of samples which were collected from dykes hosted in the oldest (Paleo- to Mesoarchean), eastern part of the Kaapvaal Craton (e.g., Eglinton and Armstrong, 2004), including two sites (NL11 and NL12) within a ca 3.0–2.9 Ga lava-sediment cover sequence (Pongola Supergroup). In general, tonalite–trondhjemite–granodiorite (TTG) gneisses predominate within the Paleoproterozoic, while a granodiorite–monzonite–syenite (GMS) suite of intrusions make up most of the Mesoarchean (Robb et al., 2006). Neoproterozoic granitoids are not directly relevant to our study, except for the fact that most SE-trending mafic dykes do not cut post-Pongola granitoids, in agreement with this swarm's syn-Pongola age (2.95 Ga; Olsson et al., 2010). The eastern Kaapvaal Craton (Fig. 1a) also includes some of the oldest (3.5–3.2 Ga) and best preserved greenstone belts in the world (Brandl et al., 2006), but these are generally too dark to provide any good contrast to the same cross-cutting mafic dyke swarms that are more readily mapped in equally old granitoids.

2.2. Dyke swarms across eastern Kaapvaal Craton

There were few precise, absolute ages on the eastern Kaapvaal Craton dykes prior to the precise U–Pb dating by Olsson et al. (2010)

and Olsson in Söderlund et al. (2010) which identified at least three separate swarms: (1) the 2.95 Ga SE-trending Badplaas swarm, (2) the 2.65 Ga E–W trending fanning Rykoppies swarm, and (3) the 1.90 Ga NE-trending Black Ridge swarm.

The oldest 2.95 Ga-old SE-trending Badplaas dyke swarm probably acted as feeders to the Pongola volcanics (e.g., Hunter and Halls, 1992), because these dykes are generally cut by post-Pongola (NeoArchean in Fig. 1a) granitoids, are orientated sub-parallel to the possible orientation of a Pongola rift, and have roughly similar compositions (Klausen et al., 2010). Consistent 2.65 Ga ages negate previous inferences suggesting that E-trending Rykoppies dykes were feeding the neighboring E–W elongated Bushveld Complex (Uken and Watkeys, 1997; Anhaeusser, 2006). Instead, this swarm appears to be radiating (Olsson et al., 2010) and probably acted as feeders to the upper (Allanridge) lava formation within the Ventersdorp Supergroup (Klausen et al., 2010). Finally, a ca. 1.90 Ga age for NE-trending Black Ridge dykes argues for a widespread magmatic event which is correlated to sills in the Waterberg Group (Hanson et al., 2004), lavas within the Soutpansberg Group (Barker et al., 2006), and even dykes and the Mashonaland sills within the juxtaposed Zimbabwe Craton (Söderlund et al., 2010; Klausen et al., 2010).

In addition to the three dated swarms that have been studied herein there are also dykes present in each area that have other trends. These potentially represent additional magmatic events (e.g., the 0.18 Ga Karoo, 1.10 Ga Umkondo, 2.05 Ga Bushveld, 2.20 Ga Ongeluk, or other events), and will be targeted in the future for precise U–Pb dating and associated petrogenetic and paleomagnetic studies.

2.3. <2.65 Ga cover rocks and tectonic/metamorphic overprint

The eastern Kaapvaal Craton is unconformably bounded by two well-preserved supergroups: (1) the 2.65–2.05 Ga (Vaalian Epoch) Transvaal Supergroup towards the west (Fig. 1a; e.g., Eriksson et al., 2006), and (2) the 325–175 Ma Karoo Supergroup across its southern and eastern extent (e.g., Johnson et al., 2006). Both supergroups are comprised of relatively thick and varied sedimentary sequences, which are capped by rapidly emplaced and extraordinarily voluminous igneous deposits; i.e., the Bushveld Complex (Cawthorn et al., 2006) and the Karoo Igneous Province (Duncan and Marsh, 2006).

It is debated, whether the Bushveld Complex was formed (1) during a northerly collision with the Zimbabwe Craton, along the Limpopo Belt, (2) in combination with more westerly subduction prior to a collision with the Congo Craton, along the Ubendian Belt and/or (3) as a plume-induced Large Igneous Province. It is, at least, superseded by the emplacement of coeval (ca. 1.90 Ga) Soutpansberg lavas (Barker et al., 2006), Waterberg-hosted sills (Hanson et al., 2004) and mafic dykes and sills across northern Kaapvaal and southern Zimbabwe Craton (Olsson, unpublished results; Söderlund et al., 2010; Klausen et al., 2010), closely followed by the ca. 1.8 Ga Eburnean orogeny. The timing of collision of the Zimbabwe and Kaapvaal Cratons along the Limpopo Belt is constrained by this magmatic record (Söderlund et al., 2010). Specifically, the apparent absence of 2.06 Ga Bushveld magmatism in the Zimbabwe Craton and the corresponding absence of 2.58 Ga Great Dyke of Zimbabwe magmatism in the Kaapvaal Craton, suggest that the Zimbabwe and Kaapvaal Cratons were still separate at these times. Furthermore, since ca. 1.90 Ga magmatism is present in both Zimbabwe and Kaapvaal Cratons, then collision and welding of these two cratons must have occurred between 1.90 Ga and 2.06 Ga.

The ca. 0.18 Ga Karoo Large Igneous Province is related to Gondwana break-up, where a vast band across South America, southern Africa and Antarctica was affected by voluminous magmatism.

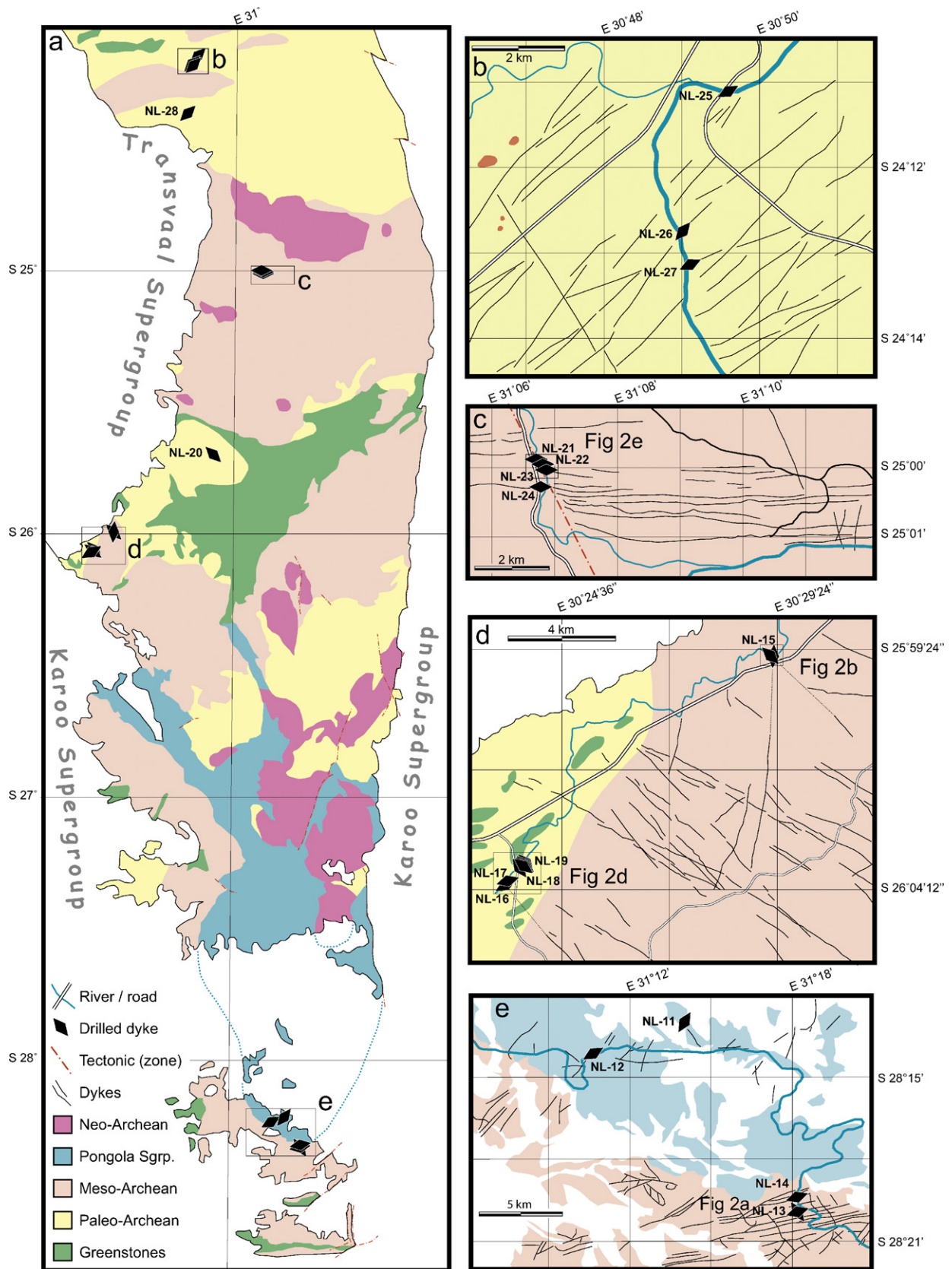


Fig. 1. Geological map of the eastern part of the Kaapvaal Craton, modified from Robb et al. (2006). More detailed maps of four target areas (b–e) are compiled from 1:250,000 geological maps, with additional dyke lineaments traced from Google Earth. Orientations of sampled dykes are indicated by black diamonds.

Thus, the eastern Kaapvaal Craton potentially hosts Jurassic (Karoo) dykes that may be difficult to distinguish from Precambrian dykes. While Karoo dykes and sills have been distinguished on geological maps as less altered, this may be an unreliable criteria. For instance, Jourdan et al.'s (2006) reconnaissance Ar/Ar-study of the NE-trending Orange River Dyke Swarm in the northeastern part of the Kaapvaal Craton revealed, contrary to map classifications, only dykes of Precambrian age. In general, however, we suspect that the following intrusions are Jurassic (1) N–S trending dykes, because these parallel the Lebombo Group monocline and hosted dyke swarms (e.g., Klausen, 2009), (2) WNW–ESE-trending dykes across the northeastern part of the Kaapvaal Craton, because these parallel the Okavango Dyke Swarm (Reeves, 2000; Jourdan et al., 2006), and (3) all sills, and potential feeders to these, near the Karoo Supergroup cover across the southern parts of the eastern Kaapvaal Craton.

Tectonic disruptions during Gondwana break-up are not believed to have significantly rotated any of our sample sites because rift related deformations concentrated along the African continent's passive margins (Klausen, 2009), while Karoo Supergroup sequences are relatively horizontal away from these margins and across most of the southern part of the eastern Kaapvaal Craton.

3. Targeted dyke swarms

Dykes were targeted within four parts of the eastern Kaapvaal Craton, in order to sample the NE-, E- and SE-trending swarms of known intrusive ages, 1.90, 2.65 and 2.95 Ga, respectively (Olsson et al., 2010; Olsson in Söderlund et al., 2010). Below, is a brief summary of some of the more important dyke and structural features within each of the four target area (Fig. 1b–e).

3.1. Black Hills dyke swarm, northeastern part of the Kaapvaal Craton (north of ~24°30'S)

Satellite imagery (e.g., Google Earth) and aeromagnetic compilations clearly reveal the predominance of NE-trending dykes, which appear to become denser towards the Jurassic Lebombo–Mwenetzi–Okavango triple-junction (e.g., Reeves, 2000; Jourdan et al., 2006; Klausen, 2009). However, only Precambrian and no Phanerozoic dykes were recorded among these in the Jourdan et al. (2006) Ar–Ar reconnaissance study. An apparent kink from a more easterly trending swarm across Kaapvaal Craton to a more northerly trend across the Transvaal Supergroup (Uken and Watkeys, 1997), is possibly an artifact of the juxtaposition of two different swarms, a more easterly trending >2.65 Ga swarm that does not cut the Transvaal Supergroup and a more northerly trending and presumed ca. 1.90 Ga swarm that does (Klausen et al., 2010). This conjugate pattern between approximately N030°E- and N060°E-trending dykes is evident throughout the northeastern part of the Kaapvaal Craton, and the older more easterly trending set of dykes is possibly more metamorphosed and, therefore, less suited for geochronology. Note that both a presumed 1.90 Ga-old N035°E-dyke and a presumed older N065°E-dyke have been sampled at sites NL-26 and NL-27, respectively (Fig. 1b).

3.2. Rykoppies dyke swarm, eastern part of the Kaapvaal Craton (~24°30'S to ~25°30'S)

East-trending dykes appear to concentrate in this part of the craton, along the axis of the E–W elongated Transvaal Supergroup (including the Rustenburg Layered Suite). Relatively few NE-, N- and SE-trending dykes appear to cross-cut this well-constrained 2.65 Ga swarm but our sample sites are located within a NNW–SSE-trending shear zone. The age of these sericitised and silicified shear zones is unconstrained (Walraven and Hartzler, 1986) but they are

oriented conspicuously sub-parallel to the 2.95 Ga-old SE-trending swarm. Such a tentative correlation may at first be discounted by the prevalent right-lateral offsets of all 2.65 Ga E-trending dykes along this shear zone, but the question is whether these systematic offsets were caused by post-intrusive tectonic shear or by propagating dykes consistently following a pre-existing shear zone in right-lateral fashion? The following observations convince us that the right-lateral offsets along these 2.65 Ga dykes are of a primary intrusive origin: (1) three cases of conspicuous dykelets – located consistently to the left of a corresponding major right-lateral offset – resemble typical “horns” extending from magmatic dyke offsets, (2) dykes do not appear nearly as sheared as the host rock, and (3) NL-23 is offset by a greater amount than NL-22 across the same fault zone (Fig. 2e). Thus, while being aware of the possibility of any secondary deformation, we are confident that samples from sites NL-21 to -23 are unaffected by this shear zone.

3.3. Badplaas dyke swarm, southeastern part of Kaapvaal Craton (25°30'S to 27°30'S)

This part of the Kaapvaal Craton has been more intensively investigated because it includes the world-famous Barberton Greenstone Belt. Remarkable high-standing SE-trending mafic dyke ridges extend across many contrasting pale granitoids, and these are believed to have been feeding Nsuze lavas within the Pongola Supergroup (e.g., Hunter and Halls, 1992; Olsson et al., 2010; Klausen et al., 2010). However, more than one age is thought to be present for the following reasons. (1) a SE–ESE-trending dyke is of comparable age to the E-trending Rykoppies swarm located further north, thus defining a fanning swarm of this age (Olsson et al., 2010), (2) SE-trending dykes may be subdivided into two geochemically different groups which may be of different ages (e.g., Hunter and Halls, 1992), and (3) in detail, SE-trending dykes have two distinct trends, ~N120°E–N150°E which would probably represent different swarms (Fig. 1b and d). In addition, there are sporadic N–S trending dykes (e.g., NL-15 in Fig. 2b) of presumed Jurassic age, and also more subdued SW–NE-trending dykes of likely 1.90 Ga (e.g., NL-16 and -17 in Fig. 2c and d).

3.4. Southeasternmost window to the Kaapvaal Craton (south of ~28°S)

This isolated window to the eastern Kaapvaal Craton exposes some less well-known Mesoproterozoic granitoids and greenstone belts, onto which the southernmost remains of Pongola Supergroup are remarkably well-preserved (Gold, 2006). A NE-trending and an E- to ENE-trending dyke swarm dominate the area. Some SE-trending dykes are also present and are likely to be southernmost outliers to the same syn-Pongola dyke swarm that is dated near Badplaas. All attempts to date dykes within this southeasternmost window have so far been unsuccessful.

Unlike the NE-dykes across the northeastern Kaapvaal Craton, NE-trending dykes in the southeasternmost window are often characteristically feldspar-phyric, and are often observed cutting through the Pongola Supergroup. E–ENE-trending dykes appear indistinguishable from those within the E-trending Rykoppies swarm and may, likewise, contain variable amounts of basement xenoliths. One E–ENE-trending and exceptionally xenolith-rich dyke is cut by a strongly feldspar-phyric NE-trending dyke (Klausen et al., 2010), while one easterly trending dyke both cuts one braided SE-trending dyke and is cut by another slightly more northerly trending and fresher looking dyke of presumed Jurassic age (NL-13 in Fig. 2e). Compared to the rest of the eastern Kaapvaal Craton, the southeasternmost window is more heavily cross-cut by a complex array of dykes and sills, which extend into the overlying Karoo Supergroup and thereby are Jurassic. Apart from the

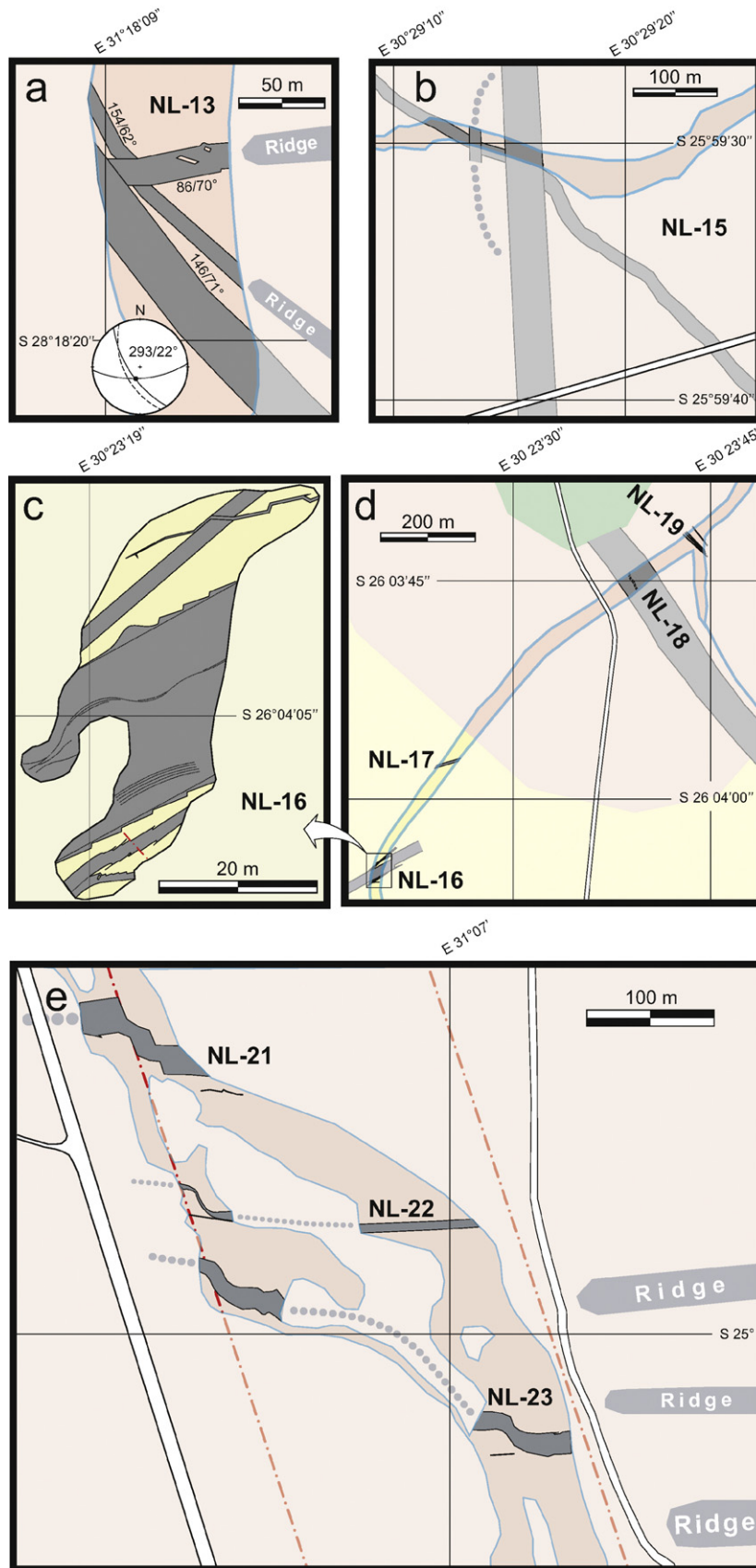


Fig. 2. Detailed field sketch maps of selected sample sites, highlighting interesting structural relationships. Stereographical diagram shows planes of all three dykes at NL-13 (oldest braided dyke plane is dashed), where the azimuth of the intersection between the two more regular dykes (solid planes) is consistent with a common 22° post-intrusive tilt of initially vertical dykes towards N013°E'.

Table 1
Location of sites and summary of paleomagnetic data for dolerite dykes of the eastern Kaapvaal Craton.

Site	Strike N°E	Dyke thickness, m	Component	Site location		Polarity	B/N	Dec (°)	Inc (°)	$\alpha_{95}(\circ)$	K	Test	Age of rock/age of magnetization (Ga)
				Latitude, °S	Longitude, °E								
Northeastern area													
NL-25	NE60	~5	M_{NE}	24.1845	30.8227	R	1/12	314.4	74.7	5.3	68.1	–	1.90/1.90
NL-26	NE35	32	M_{NE}	24.2124	30.8167	R	3/16	320.2	58.2	5.8	41.4	C ⁺	1.90/1.90
NL-27	NE65	18	M_{NE}	24.2193	30.8180	R	2/15	310.3	56.3	6.2	39.0	–	1.90/1.90
NL-28	NE57	m.b. sill	M_{NE}	24.4056	30.7975	N	1/9	141.7	–67.6	6.0	73.6	–	1.90**/1.90
Northeastern area, mean directions for Black Hills swarm (1.90 Ga)													
Mean for samples			M_{NE}	24.3	30.8	N+R	52	136.1	–63.2	3.4	35.4	–	1.90/1.90
Mean for sites			M_{NE}	24.3	30.8	N+R	4*/8	136.4	–61.5	5.6	98.1	–	1.90/1.90
Eastern area													
NL-20	E117	13	H_{EW}	25.7025	30.9163	R	2/13	210.7	61.0	7.9	33.0	C ⁺	2.65**/2.65
NL-21	E90	15	H_{EW}	24.9983	31.1149	R	3/13	201.9	60.2	7.5	31.8	C ⁺	2.65/2.65
NL-22	E90	1.5–2	H_{EW}	24.9993	31.1166	R	2/9	202.4	52.9	10.3	25.9	–	2.65/2.65
NL-23	E90	15	H_{EW}	25.0007	31.1174	R	3/16	215.7	58.2	6.3	37.2	–	2.65/2.65
NL-24	E90	15	H_{EW}	25.0045	31.1155	Chaotic distribution							2.65**/UN
Eastern area, mean direction for Rykoppies swarm (2.65 Ga)													
Mean for samples			H_{EW}	25.0	31.1	R	52	207.3	57.7	3.5	28.5	C ⁺ , R ⁺	2.65/2.65
Mean for sites			H_{EW}	25.0	31.1	R	5*/10	207.5	58.2	5.8	253.7	C ⁺ , R ⁺	2.65/2.65
Southeastern area													
NL-15	SE135	10	P_{SE}	25.9914	30.4866	N	2/8	209	31.4	11.1	25.9	–	2.95/2.95
			M_{SE}			N	1/4	155.4	–55.9	22.0	18.5	–	2.95/1.90
NL-15 (thin)	N180	3–5	K_{SE}	25.9917	30.4870	R	1/5	331.4	–55.6	14.4	29.3	–	0.18/0.18
NL-16a	NE60	1.5–2	M_{SE}	26.0678	30.3889	N	2/7	124.5	–65.6	10.4	34.7	–	1.90/1.90
NL-16b	NE50	0.5–1	N_{SE}	26.0678	30.3889	N	1/6	71.8	37.7	17.3	16.0	–	UN/2.15/UN
NL-16c	NE70	0.2	K_{SE}	26.0678	30.3889	R	1/7	332.1	–21.9	13.7	20.0	–	1.90/0.18
NL-17	NE75	3–4	M_{SE}	26.0659	30.3903	N	1/9	117.9	–44.6	14.5	13.6	–	1.90/1.90
NL-18	SE144	~40	K_{SE}	26.0622	30.3945	R	1/4	322.9	–30.8	16.2	33.1	–	2.95/0.18
NL-19 (thin 1–4)	SE130–140	0.35–0.4	P_{SE}	26.0618	30.3955	N	4/11	205.2	33.5	27.5	8.9	–	2.95/2.95
Southeastern area, mean direction for Badplaas swarm (2.95 Ga)													
Mean for sites			P_{SE}	26.0	30.4	N	2*/6	207.4	32.5	9.3	721.9	–	2.95/2.95
Mean for samples				N	19	207.1	32.6	6.5	27.8	–			
Southeastern area, mean direction for Black Hills swarm (1.90 Ga)													
Mean for sites			M_{SE}	26.1	30.4	N	3*/4	131.8	–56.5	24.1	27.3	–	2.95–1.90/1.90
Mean for samples				N	20	126.8	–55.2	9.1	13.9	–			
Southeastern area, mean direction for Karoo remagnetization (0.18 Ga)													
Mean for sites			K_{SE}	26.1	30.4	R	3*/3	328.6	–36.1	28.0	20.5	–	2.95–0.18/0.18
Mean for samples				R	18	329.5	–32.3	9.9	15.0	–			
Southeasternmost area													
NL-11	NE50	10?	M_{SEM}	28.2167	31.2403	N	1/14	136.5	–38.6	7.5	27.0	C ⁺	1.90/1.90
NL-12	NE50	11	M_{SEM}	28.2356	31.1791	R	2/11	275.7	35.4	7.2	40.6	C ⁺ , G	1.90/1.90
		Flood basalts	NB	28.2356	31.1791	N	3/10	203.6	36.1	7.9	38.5	C ⁺ , G	2.95/2.95
NL-13a (oldest)	SE135	9	P_{SEM}	28.3323	31.3028	N	2/8	208.8	34.3	9.4	35.7	–	2.95/2.95
NL-13b	E85	15	H_{SEM}	28.3323	31.3028	N	1/7	229.2	62.2	13.8	20.1	C ⁺ , R ⁺	2.65/2.65
						R	1/8	34.0	–57.6	8.3	45.7		
						N+R	2/15	220.5	59.9	7.3	28.3		
						Angular separation $\gamma = 8.87^\circ$ with critical separation E95% $\gamma_c = 14.62^\circ$							
NL-13c (youngest)	SE145	32	K_{SEM}	28.3323	31.3028	R	1/10	297.1	–32.0	6.8	51.1	–	0.18/0.18
NL-14	E80	28	H_{SEM}	28.3235	31.3025	N	2/5	200.2	45.7	8.5	82.0	–	2.65/2.65
Southeasternmost area, mean directions for Badplaas swarm (2.95 Ga)													
Mean for sites			$NB + P_{SEM}$	28.3	31.3	N	2*/5	206.2	35.2	10.1	616.9	C ⁺ , G	2.95/2.95
Mean for samples							18	205.9	35.3	5.7	38.4		

Southeasternmost area, mean directions for Rykkoppies (?) swarm (2.65 Ga?)											
Mean for sites											
Mean for samples											
Mean directions for the different dyke swarms of the Kaapvaal Craton											
Mean for the Badplaas swarm (2.95 Ga)											
Mean for Rykkoppies swarm (2.65 Ga)											
Mean for Black Hills swarm (1.90 Ga)											
Mean for Karoo remagnetization (0.18 Ga)											
	H_{SEM}	28.3	31.3	N + R	2°/4	208.7	53.7	41.7	38.0	C ⁺ , R ⁺	2.65/2.65
	<i>P</i>		Samples	N	37	206.5	33.9	4.2	32.7	C ⁺ , G	2.95/2.95
	<i>H</i>		Sites	N + R	4	206.8	33.8	3.5	695.3	C ⁺ , R ⁺	2.65/2.65
			Samples	N + R	71	209.1	57.4	3.3	27.4	C ⁺ , R ⁺	
			Sites	N + R	7	210.4	56.6	6.9	78.5	R ⁺	2.95–1.90/1.90
	<i>M</i>		Samples	N + R	83	125.6	–58.6	3.9	16.6	C [–]	2.95–0.18/0.18
			Sites	R	8	126.9	–58.7	11.5	24.2		
	<i>K</i>		Samples	R	16	329.5	–34.7	10.3	14.3		
			Sites		3	328.3	–36.1	28.0	20.5		

Notes: B/N: number of sites/samples; Dec, Inc: site-mean declination, inclination; K: precision parameter of Fisher (1953); α_{95} : semi-angle of 95% cone of confidence about mean direction; R⁺: positive reversal, C⁺: positive contact tests; UN: unknown age; *: number of localities; **: dyke site with U–Pb baddeleyite age obtained by Olsson et al. (2010) and Olsson in Söderlund et al. (2010).

presumed Jurassic SE-dyke at NL-13, the above cross-cutting relationships between SE, ESE and NE-trending dykes are consistent with the 2.95, 2.65 and 1.90 Ga ages, respectively, constrained for similar trending dykes farther to the north (see also Klausen et al., 2010).

Apart from some local complexities that are poorly constrained, well-preserved bedding planes within the Pongola Supergroup generally map out a large open fold across the area, commonly with gentle (10–20°) dips towards the NE to N. The Pongola host can thereby be used to restore the subsequent tilting of the drilled NE-dykes at NL11–12. This post-Pongola regional tilt also explains a more precisely estimated 22° of apparent post-intrusive tilt towards N013°E, recorded by the two younger dykes at NL-13 (cf., inset stereographical diagram in Fig. 2a), while the maximum age of this tilting hinges on the absolute age of the youngest (possibly Jurassic) SE-dyke.

4. Paleomagnetic and AMS studies

A paleomagnetic and anisotropy of magnetic susceptibility (AMS) study has been applied to various dolerite dyke swarms across the Kaapvaal Craton. 431 oriented samples were collected at 15 sites in the NE, E, and SE regions to the east of the Bushveld Igneous Complex, representing swarms of ages 1.90, 2.65 and 2.95 Ga, respectively (Olsson et al., 2010; Söderlund et al., 2010; Olsson in Söderlund et al., 2010). At each site (Table 1), about 10–20 oriented samples were collected from each dyke and about 5–10 samples from a host rock that most often was a granitoid–granodiorite of either Palaeoarchean or Mesoarchean age, as indicated in Figs. 1 and 2. In the most southeasterly positioned area, samples from a ~2.95 Ga-old Nsuze basalt lava host (Pongola Supergroup) at site NL-12 and an overlying ~0.18 Ga-old Karoo sill at site NL-13 were also collected for baked-contact tests. In addition a conglomerate test was done at site NL-12.

AMS is a sensitive tool for determining the rock fabric and it relies on magnetic minerals to produce a fabric which can be measured (e.g., Hrouda, 1982; Tarling and Hrouda, 1993). For dolerite dykes and sills, the magnetic fabric is caused by magnetite–titanomagnetite, and the resulting fabric can be reflective of magma flow. Applied to dyke swarms, it allows determination of whether regional flow is dominantly vertical or horizontal. AMS studies (e.g., Ernst and Baragar, 1992) have demonstrated that regional dyke swarms exhibit vertical flow close to their plume centers and horizontal flow away from the plume centers for distances of over 2000 km. It is also possible to determine the polarity of magmatic flow by comparing the AMS fabric of near margin samples with the local trend of the margin in order to identify an imbrication reflecting a subtle shingling of plagioclase grains in the near margin region similar to pebble imbrication in a flowing stream (Knight and Walker, 1988). Complications are possible in which the maximum susceptibility axis is not aligned with the flow direction. This can theoretically occur when single domain (vs. multidomain) magnetite grains contribute significantly to the magnetic fabric (e.g., Potter and Stephenson, 1988; Rochette et al., 1999), but in dolerite sill provinces and dyke swarms these complications are probably generally subordinate (e.g., Palmer et al., 2007). In the present study we wish to determine the flow pattern (vertical or horizontal) in each regional swarm, and potentially the flow polarity using the imbrication effect.

4.1. Methods

Four hundred and thirty-one samples were collected from 27 doleritic dykes with predominantly SE, EW, and NE trends, as well

NORTHEASTERN AREA

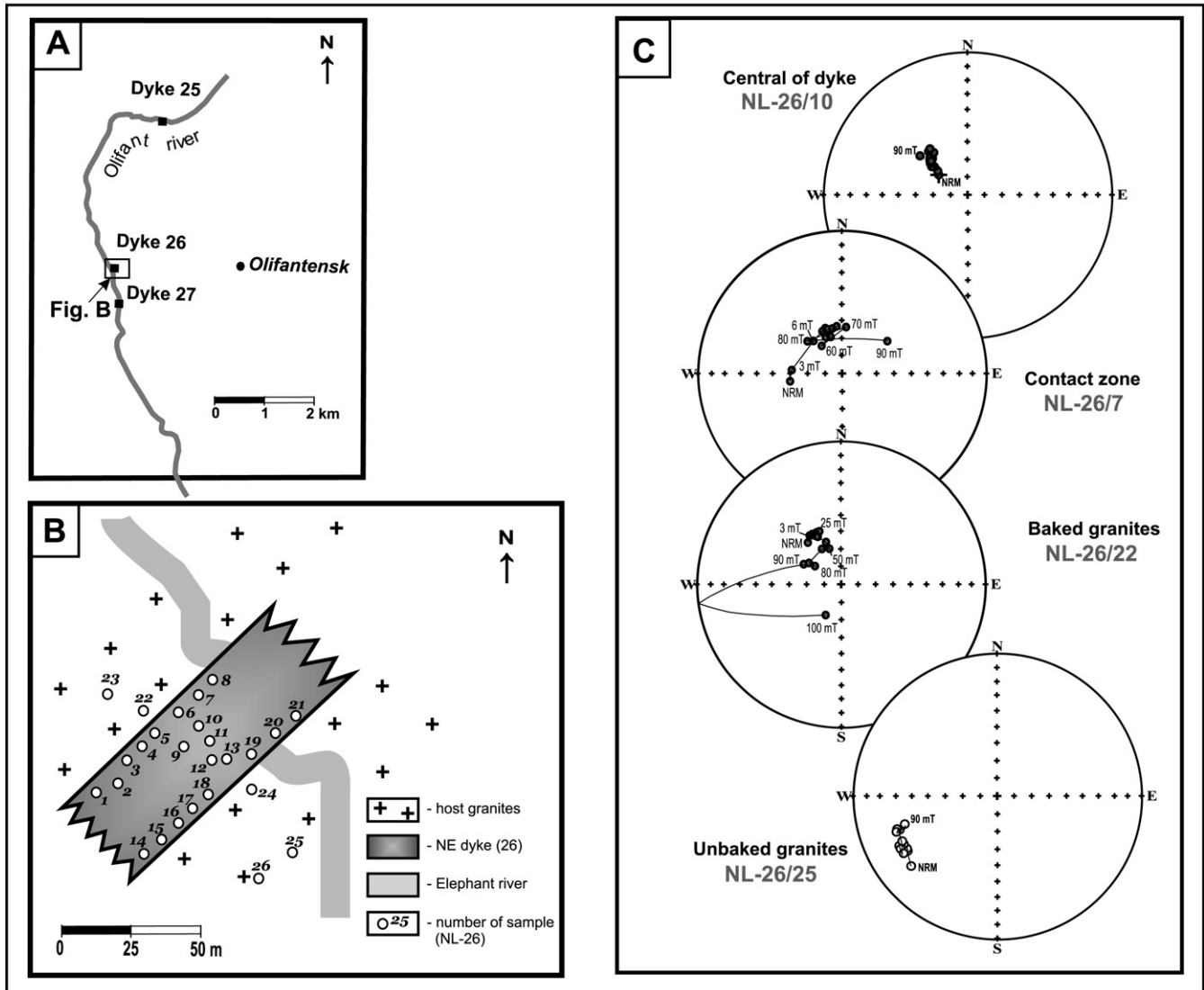


Fig. 3. Distribution of samples at sites NL-25, -26 and -27 (northeastern area). (A) Site locations along Elephant River. (B) Detailed site map at NL-26 for baked-contact test. (C) Stereonet plots of sample behavior under demagnetization for the baked-contact test. In this and all subsequent paleomagnetic diagrams solid (open) symbols are plotted on lower (upper) surface of equal-area stereonet.

as host granitoids, granodiorites, Nsuzé basalts and conglomerates (Table 1). Some of the samples were collected using a water-cooled portable drill and the remainder were collected as block samples. All samples were oriented with both a magnetic and sun compass. There were no significant differences between sun and magnetic compass orientation measurements.

4.1.1. Paleomagnetic studies

The drill core samples were cut into standard cylinders and the block samples were sawed into cubes of 2 cm × 2 cm × 2 cm in size. Part of the collection was measured at the palaeomagnetic laboratory of Lund University (LU), Sweden and part at the petromagnetic laboratory of Moscow State University (MSU), Russia. Remanence measurements were performed using a 2G cryogenic magnetometer (LU) and a JR-6 spinner-magnetometer (MSU). Conventional progressive thermal or alternating field (AF) demagnetization was applied to all specimens. Demagnetization generally consisted of 15–30 steps. Chemical changes during thermal cleaning were monitored by measuring the magnetic sus-

ceptibility after each heating step using a KLY-4S Kappabridge instrument.

NRM components were visually identified by using stereographic and orthogonal projections (Zijderveld, 1967). The directions of components were calculated according to the principal component analysis method (Kirschvink, 1980). Only components with a maximum angular deviation (MAD) less than 5° were accepted for further interpretation. Mean directions were calculated according to Fisher (1953). All calculations and graphic representations of the results were performed using software by Enkin (1994) and Chadima et al. (2004).

4.1.2. AMS studies

The anisotropy of the weak field magnetic susceptibility (AMS) was measured for one specimen from each sample using the KLY-4S instrument (e.g., Elming and Mattsson, 2001; Hrouda, 1982). The anisotropy of magnetic susceptibility (AMS) of a rock is controlled by the orientation, partly by the distribution of ferromagnetic minerals and to a lesser extent by the orientation

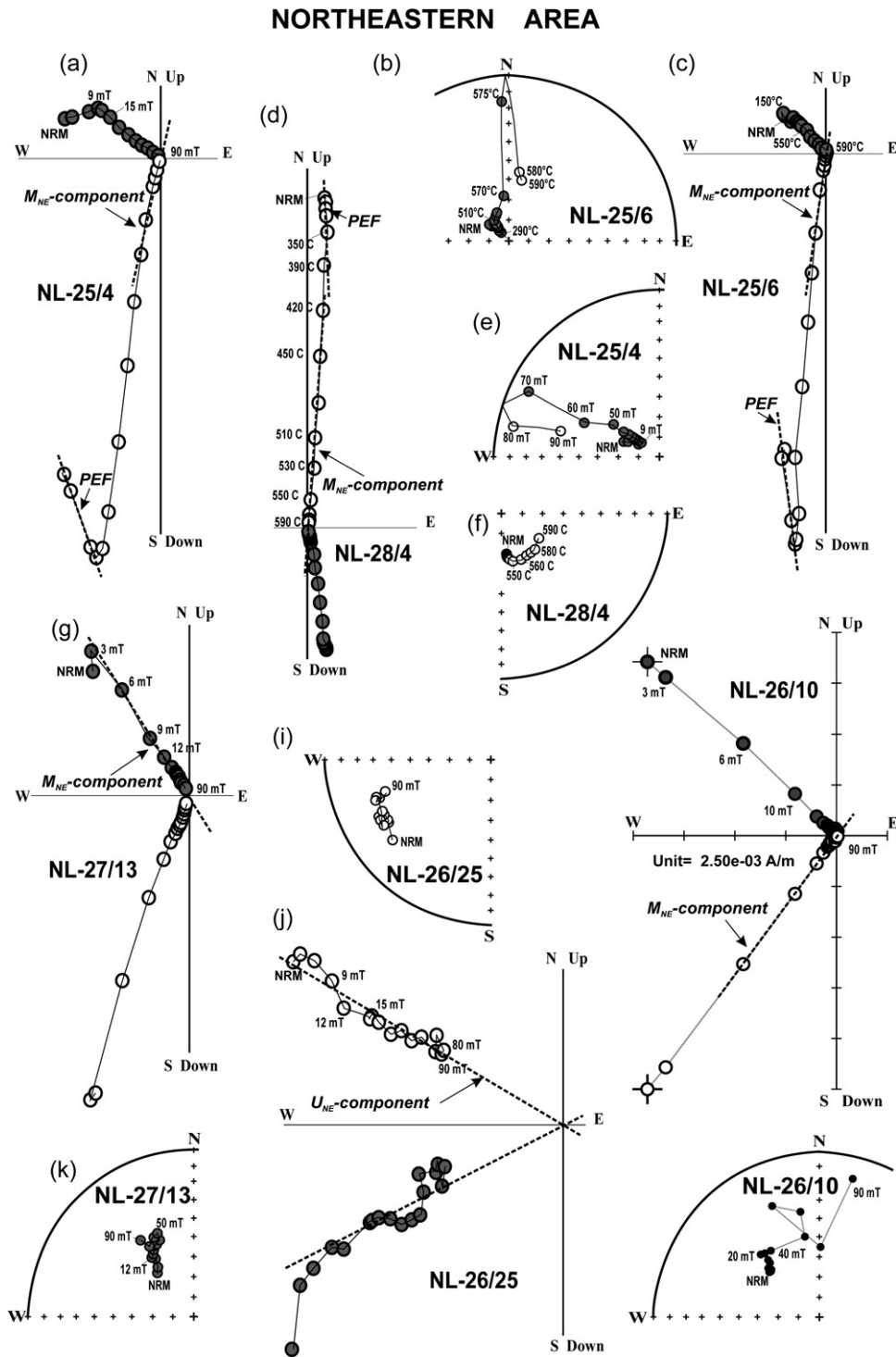


Fig. 4. Examples of AF and thermal demagnetization behavior of specimens from the NE-trending dolerite dykes from the northeastern area: (a–h) four examples: NL-26/9, NL-25/4, NL-25/6 and NL-28/4, from the dolerite dykes; (i–j) sample NL-27/13, baked host granites; (k–l) unbaked granite-gneiss of the host Pongola Formation.

of paramagnetic minerals (Tarling and Hrouda, 1993). Multiple measurement of the susceptibility in a variety of orientations in a sample allows for the definition of a susceptibility ellipsoid with three principal susceptibility axes: with maximum (K_1), intermediate (K_2), and minimum (K_3) directions and magnitudes. These principal susceptibilities, K_1 , K_2 and K_3 , are also used to derive alternative combinations of magnitude parameters such as the bulk susceptibility, $K_{\text{mean}} = (K_1 + K_2 + K_3)/3$, the degree of magnetic lineation ($L = K_1/K_2$) and the degree of magnetic foliation ($F = K_2/K_3$). The degree of anisotropy is given by $P = K_1/K_3$,

and a value of $P=1$ describes a perfectly isotropic fabric; a P value of 1.15 describes a sample with 15% anisotropy, and so on. The shape parameter ($T = [2 \ln(K_2/K_3)] / (\ln(K_1/K_3)) - 1$) (Jelinek, 1981) is a quantitative measure of the shape of the susceptibility ellipsoid, ranging from +1 where purely foliated (oblate) to -1 where purely lineated (prolate). Other combinations of the principal susceptibility axis magnitudes can be used (e.g., the $A\%$ and $B\%$ values of Cañón-Tapia, 1994) but have essentially equivalent interpretations to the P and T parameters we are using herein.

NORTHEASTERN AREA

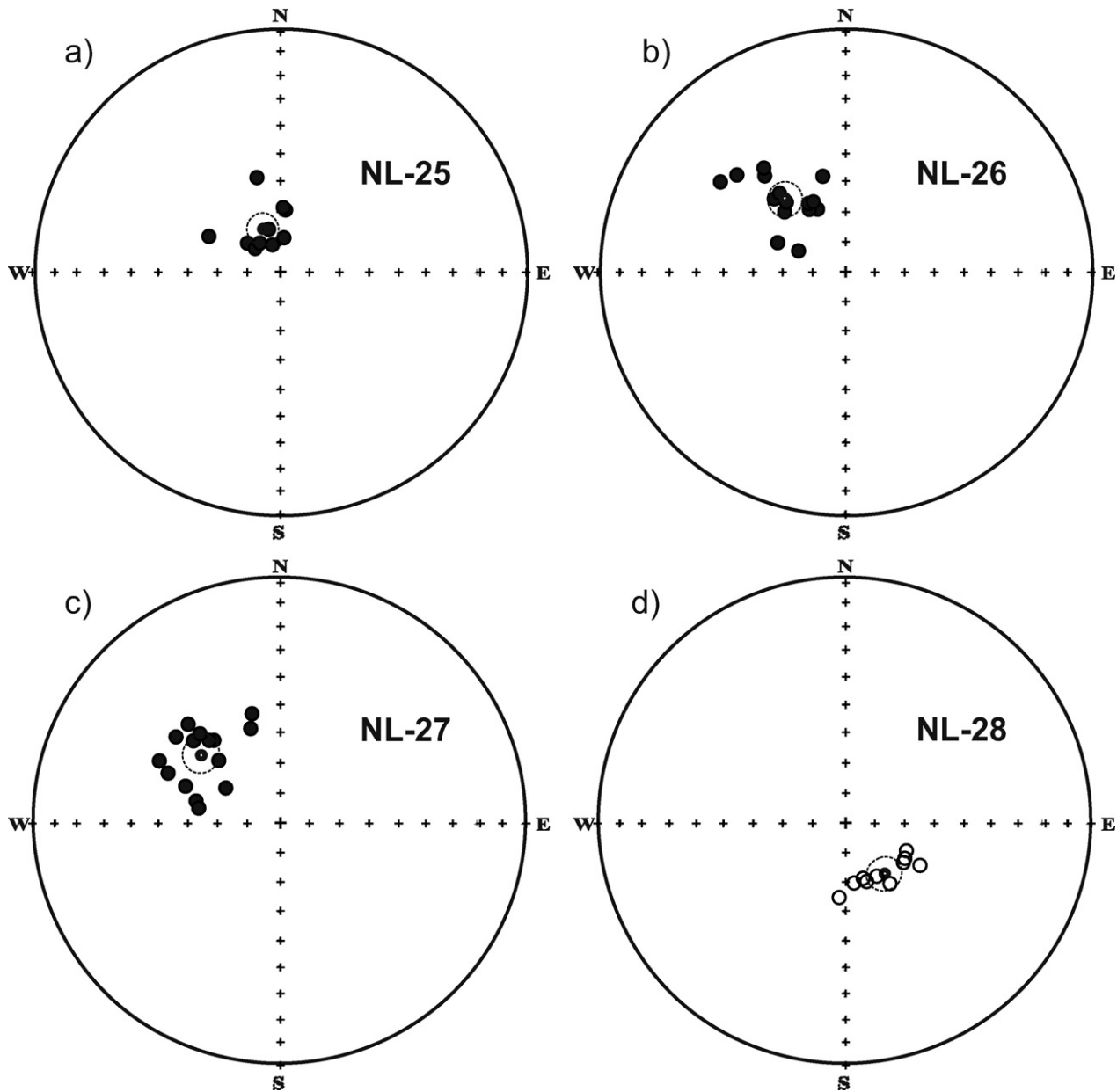


Fig. 5. Sample mean palaeomagnetic directions for the NE-trending dolerite dykes from the northeastern area. Each site mean direction is shown as a smaller dashed circle with its size given by the α_{95} confidence cone about the mean.

5. Paleomagnetic results

Paleomagnetic results from the studied dykes are summarized in Table 1. Examples of demagnetization behaviors and summaries of the remanent magnetization components are shown in Figs. 3–16.

5.1. Northeastern area (NE-trending Black Hills dykes)

Three sites (NL-25, -26 and -27) were collected along the Olifant River, each from a different NE-trending dyke (Fig. 1) and one NE-trending dyke (NL-28) was sampled along a road cut, south of the river section. One U–Pb baddeleyite age from NL-28 gives an age of

1865 Ma (Olsson, unpublished results), close to the general 1.90 Ga age attached to the Black Hills dyke swarm (Olsson in Söderlund et al., 2010). Samples for baked-contact tests for one of the sites were obtained from the host basement granites.

Each sample has two well-defined and consistent components (see Figs. 3 and 4). From NRM to about 250 °C or in alternating field below 10 mT, a direction similar to the present-day geomagnetic field (PEF) is interpreted as a VRM with very minor goethite contributions (Fig. 4a–c and e). The second remanence component, M_{NE} with dual polarity, was demagnetized in high temperatures up to 590 °C and AF fields above 10 mT. The normal polarity component M_{NE} points to the SE with negative steep-moderate inclinations (for example, sample NL-28/4 in Fig. 4d and f), and the reversed polar-

EASTERN AREA

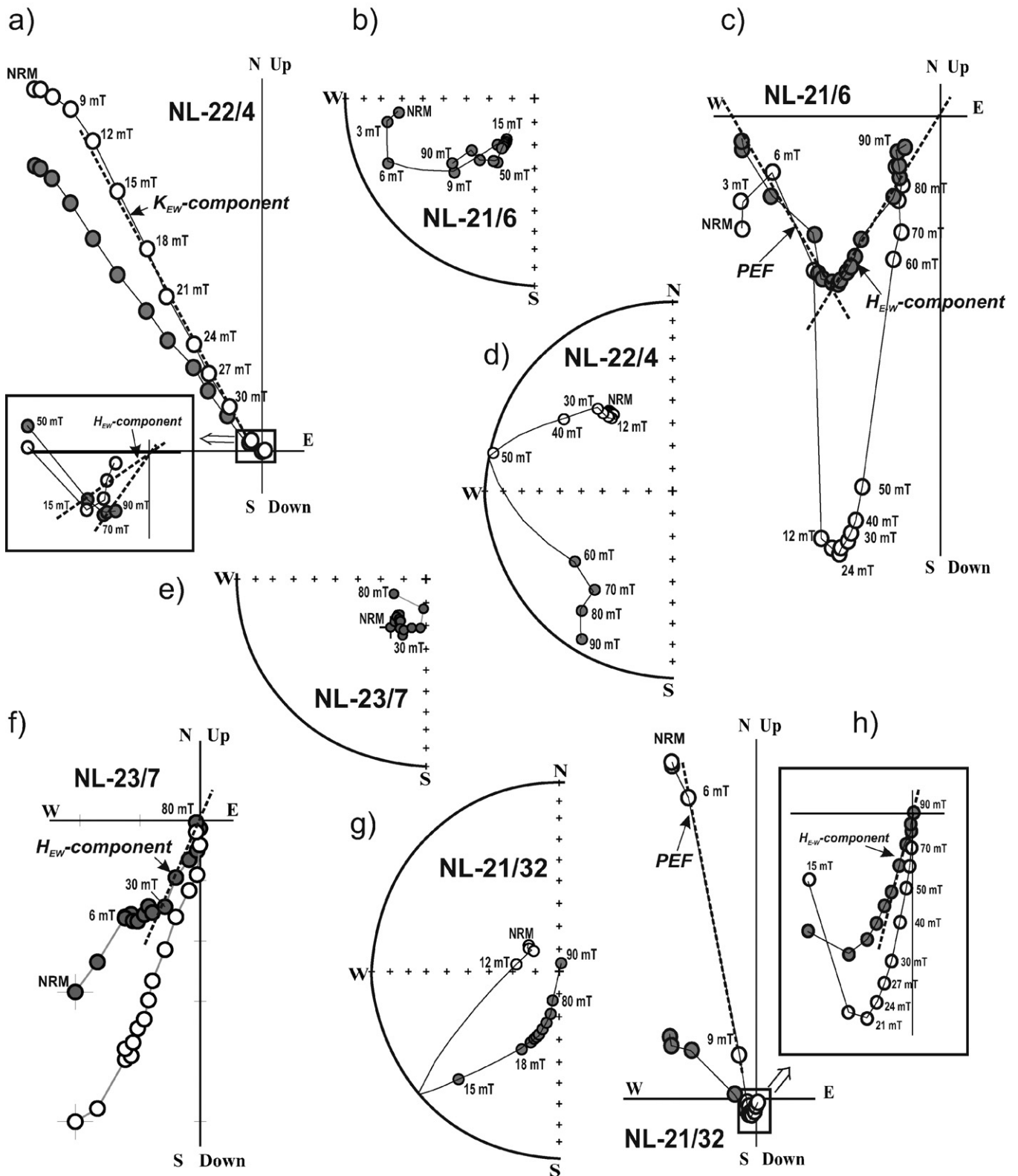


Fig. 6. Examples of thermal and AF demagnetization behavior of specimens from the E-W trending dykes of the eastern area.

EASTERN AREA

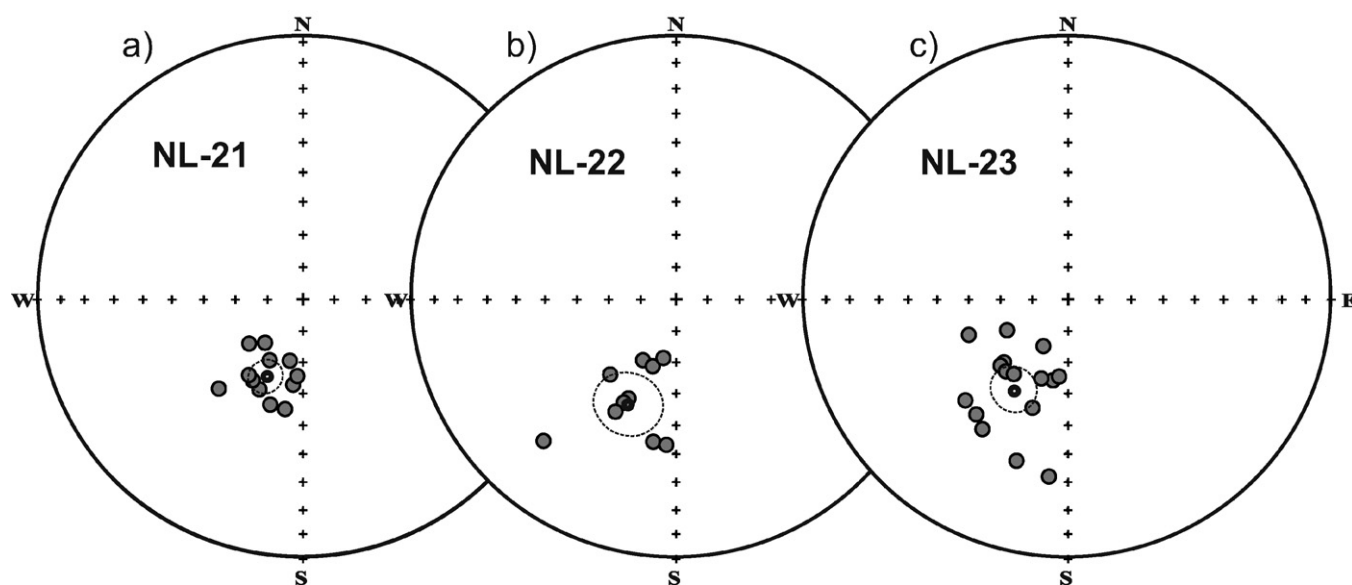


Fig. 7. Sample mean palaeomagnetic directions for the E–W trending dykes of the eastern area. Each site mean direction is shown as a dashed circle with its size given by the α_{95} confidence cone about the mean.

ity component points to the NW with positive inclination (samples NL-26/10, NL-25/4, NL-25/6 and 27/13 in Fig. 4). Samples from the NE-trending dyke at localities 25, 26 and 27 carry only a reversed polarity component, and at locality NL-28—only a normal polarity component. The normal and reverse polarity of M_{NE} component may be caused by a little bit different ages of dykes (site NL-25, NL-26 and NL-27) and sill (site NL-28). The normal and reversed directions are antipodal (Fig. 4): angular separation γ is 6.69° with critical separation γ_c 10.82° (McFadden and McElhinny, 1990).

5.2. Baked-contact test

Baked-contact tests were attempted at sites NL-25, -26 and -27. Only the test at NL-26 gave an unambiguous result. Sample NL-26/10 (Figs. 3 and 4) taken from the central part of dyke yields a steep NW directed with positive inclination, single stable remanent magnetization component. Sample NL-26/7 taken from the dyke margin has NW and downward pointing (i.e., positive inclination) direction, which is similar to the NW-pointing high-coercivity remanence direction in sample 26/22 from the baked granite (Fig. 3C). Sample NL-26/25 from the unbaked granites yields, under high AF demagnetization, a SW and upward pointing (i.e., negative inclination) direction (U_{NE} -component, Fig. 4i and j), which is clearly different from the previously discussed NW-pointing direction (Fig. 3C).

Based on the positive contact test for the NE-trending dykes, the SE-pointing steep-moderate inclination remanence direction is interpreted to be of primary origin. For the mean directions of this component, see Table 1 and Fig. 5.

5.3. Eastern area (radiating E- to SE-trending Rykoppies dykes)

One SE-trending 2.65 Ga dyke was sampled near Barberton (Fig. 1a; site NL-20). Still Farther north ($\sim 25^\circ$ S), four E–W trending dykes from the 2.65 Ga Rykoppies swarm were collected at sites NL-21 to -24 (Fig. 1a). Samples were primarily collected along the margins of each dyke. U–Pb baddeleyite ages were obtained by

Olsson et al. (2010) from various parts of this swarm, ranging from 2662 to 2686 Ma. The relatively close grouping of all these ages suggests only one swarm is present, and together the E-trending dykes and the SE-trending dyke suggest a radiating swarm is present (Olsson et al., 2010).

During stepwise thermal and alternating field (AF) demagnetization experiments, three components of NRM were isolated in the majority of specimens. A low temperature/coercivity component interpreted as the PEF (present Earth's field) is sometimes present. It is of single polarity and is directed to the northwest with steep negative (upwards) inclination. It is isolated in the temperature interval up to 250°C or in alternating field below 15 mT (Fig. 6). This component is aligned with the present-day field direction. The second remanence direction, K_{EW} -component has a single polarity which is removed at high temperatures up to $380\text{--}450^\circ\text{C}$ and AF fields below 40 mT (Fig. 6). This component points to the NW with negative moderate-shallow inclination (for example, sample NL-22/4, Fig. 6a and d). Three remaining sites have a similar, consistent H_{EW} component which points to the SW with moderate-steep positive (downwards) inclination (Table 1; Figs. 6 and 7). For the mean directions of this component (see Table 1 and Fig. 7).

5.3.1. Baked-contact test

A baked-contact test was attempted at all three localities (NL-21, -22 and -23). We sampled within the backed contact zone, and host rock granites were collected about 5–10 m away from the dykes. However, only the test from NL-21 gave a clear result. Samples NL-21/1 taken from the dyke and sample NL-21/20 taken from the chilled margin of this dyke yields a steep SW directed with steep positive inclination, single stable remanent magnetization H_{EW} component (Fig. 6a–d). Samples of baked granite contain one south-western downward P_{EW} -component of NRM (Fig. 8e and f) with unblocking temperatures of about 560°C and AF fields up to 90 mT. In samples of the unbaked granites ~ 50 m away from the dyke one high temperature/coercivity UB-component is identified. This component points to the SW with shallow negative inclination (sample NL-21/34).

EASTERN AREA CONTACT TEST

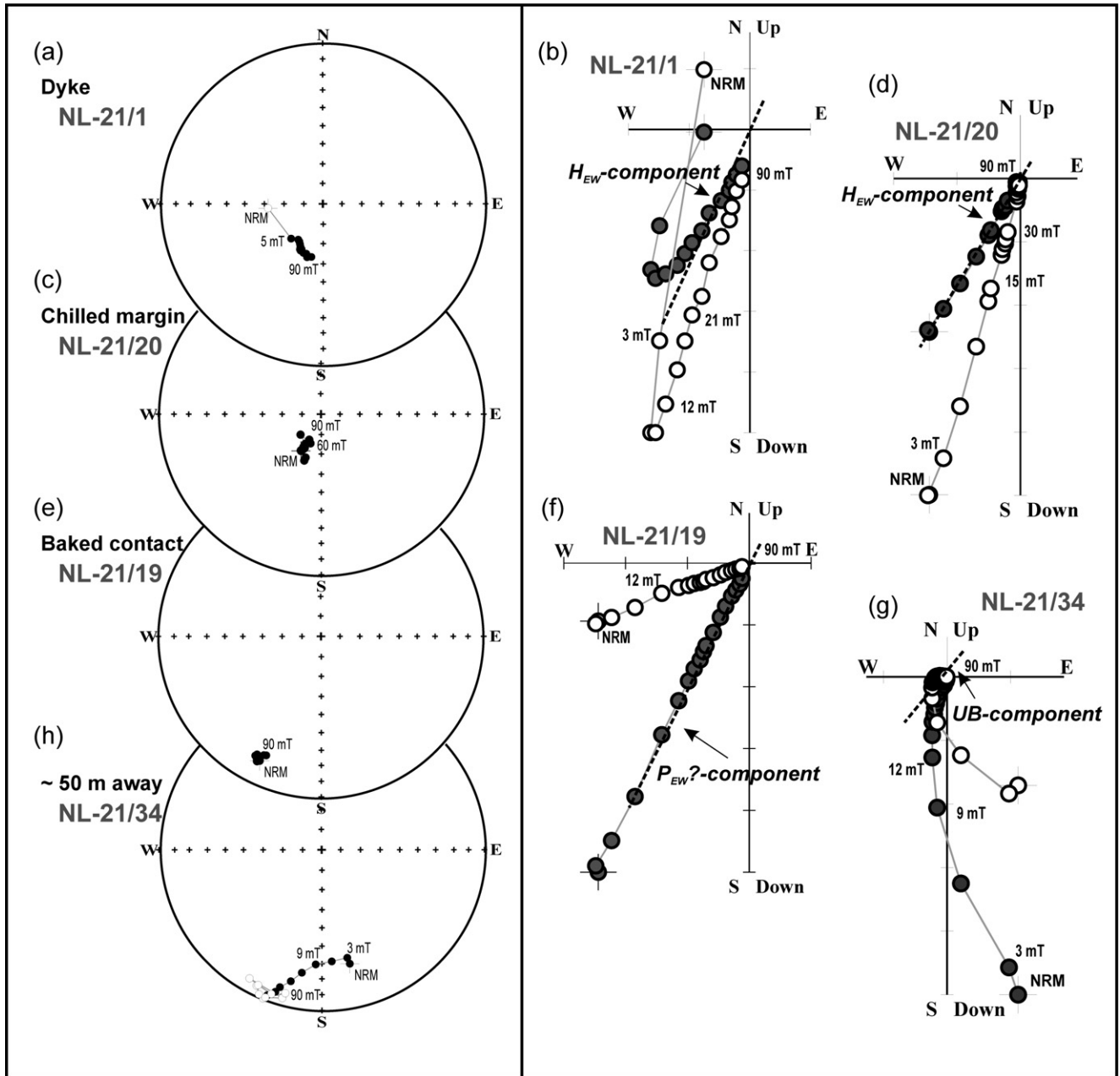


Fig. 8. Baked-contact test in the contact zone of site NL21 (eastern area, Rykoppies swarm).

Based on the positive contact test, the H_{EW} component is interpreted to be of primary origin. For the mean directions of this component (see Table 1 and Fig. 7).

5.4. Southeastern area (SE-, NE- and N-trending dykes)

Many dykes were sampled along the Buffelspruit stream, in two different localities separated by ~10 km (Fig. 1d). The first group consists of two N-trending dykes (possibly parts of the same dyke) that cut a member of the SE-trending and presumed 2.95 Ga Badplaas dyke swarm (site NL-15, Fig. 2b). The second group includes two thicker and orthogonally orientated (SE- and NE-trending)

dykes, and a number of narrower but equally SE- and NE-trending dykes, which were all sampled along a ~300 m long section of the stream (NL-16 to -19; Fig. 2d). The two thick dykes both exhibit flow and possible *in situ* crystal accumulation textures (banding indicated in Fig. 2c). A baked-contact test was attempted at all sites.

Thermal and AF demagnetization of dykes indicate the presence of two magnetic phases that, based on unblocking temperatures, are probably low-titanium titanomagnetite or magnetite (demagnetized between 520 and 590 °C) and titanomaghemite (unblocking temperatures 330–370 °C), respectively.

The SE-trending dykes from the presumed 2.95 Ga Badplaas swarm exhibit three different magnetization components. The

SOUTHEASTERN AREA

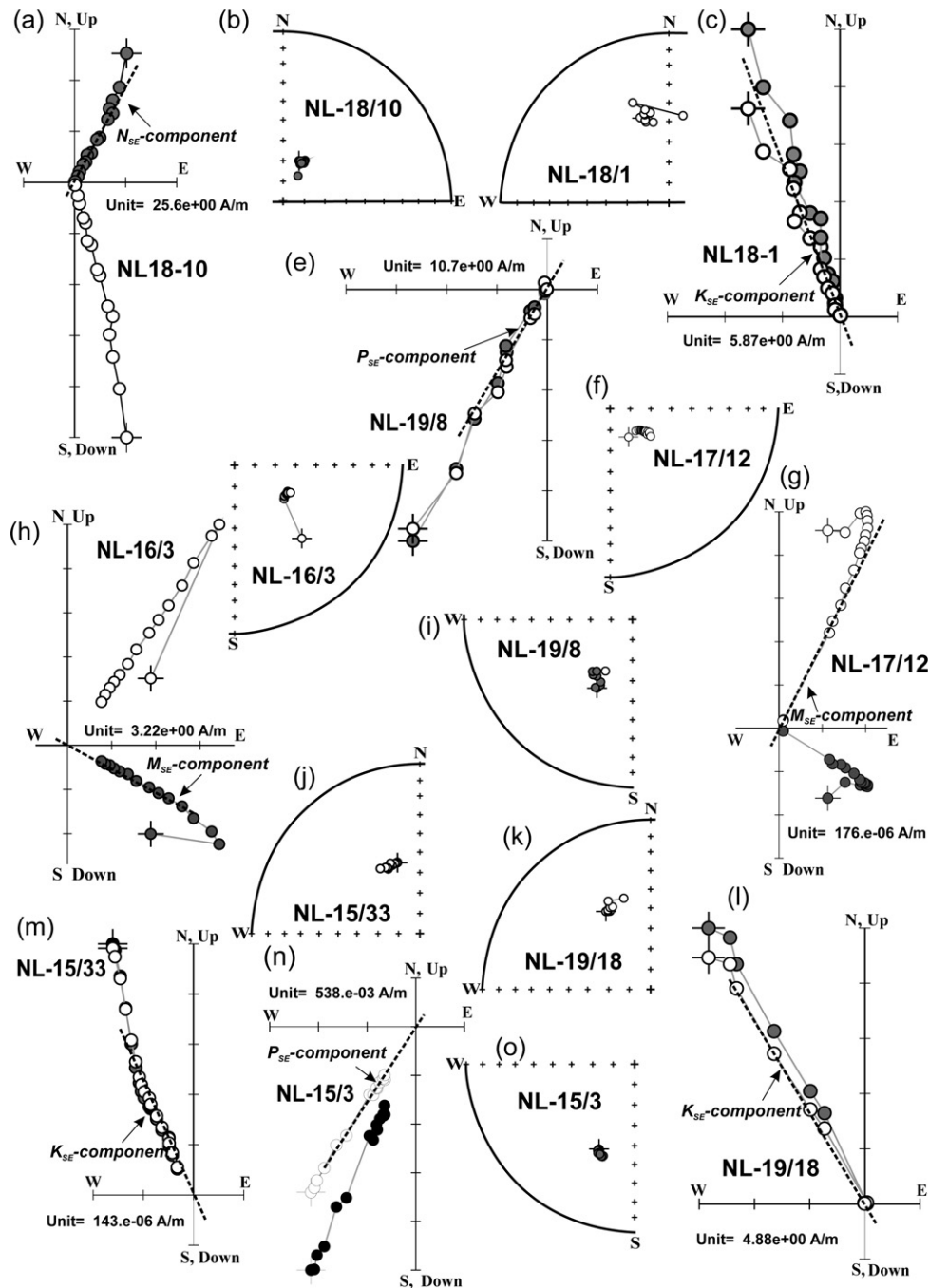


Fig. 9. Examples of paleomagnetic data from sites in the southeastern area).

first one, P_{SE} -component, characterizes samples from the contact zones, has south-southwestern declination and intermediate positive inclination (e.g., NL-15/3 and NL-19/8, Fig. 9n, o and e, i, respectively). The mean direction of this P_{SE} -component for each site is given in Table 1 and Fig. 10. The second direction characterizes samples from the 15b thin dyke of N-trend and most of the samples from the dykes at site 18 (Table 1). This K_{SE} -component has one polarity with NW declination and intermediate-steep negative inclination (e.g., sample NL-18/1, Fig. 9c and d, sample NL-19/18, Fig. 9k, l and sample NL-15/33, Fig. 9j and m). The mean direction of this component is given in Table 1 and Fig. 10a and d.

Three different high-temperature components characterize the NE-trending dykes, which potentially are all members of a very extensive 1.90 Ga Black Hills swarm (e.g., Klausen et al., 2010). The first K_{SE} -component has north-northwest declination and shallow-intermediate negative inclination. It is mostly found in samples from dyke 16c (Fig. 10d). The second M_{SE} -component is found in dykes 16a and 17 (sample NL-17/12 and NL-16/3, Fig. 9f–i). This M_{SE} -component has a SE-declination and an intermediate-steep negative inclination (mean direction in Table 1, Fig. 10c and e). The third direction, present in dyke 16b, is close to the N_{SE} -component discovered in NW-trending dykes of this area (Fig. 9a and b). This component has ENE-

SOUTHEASTERN AREA

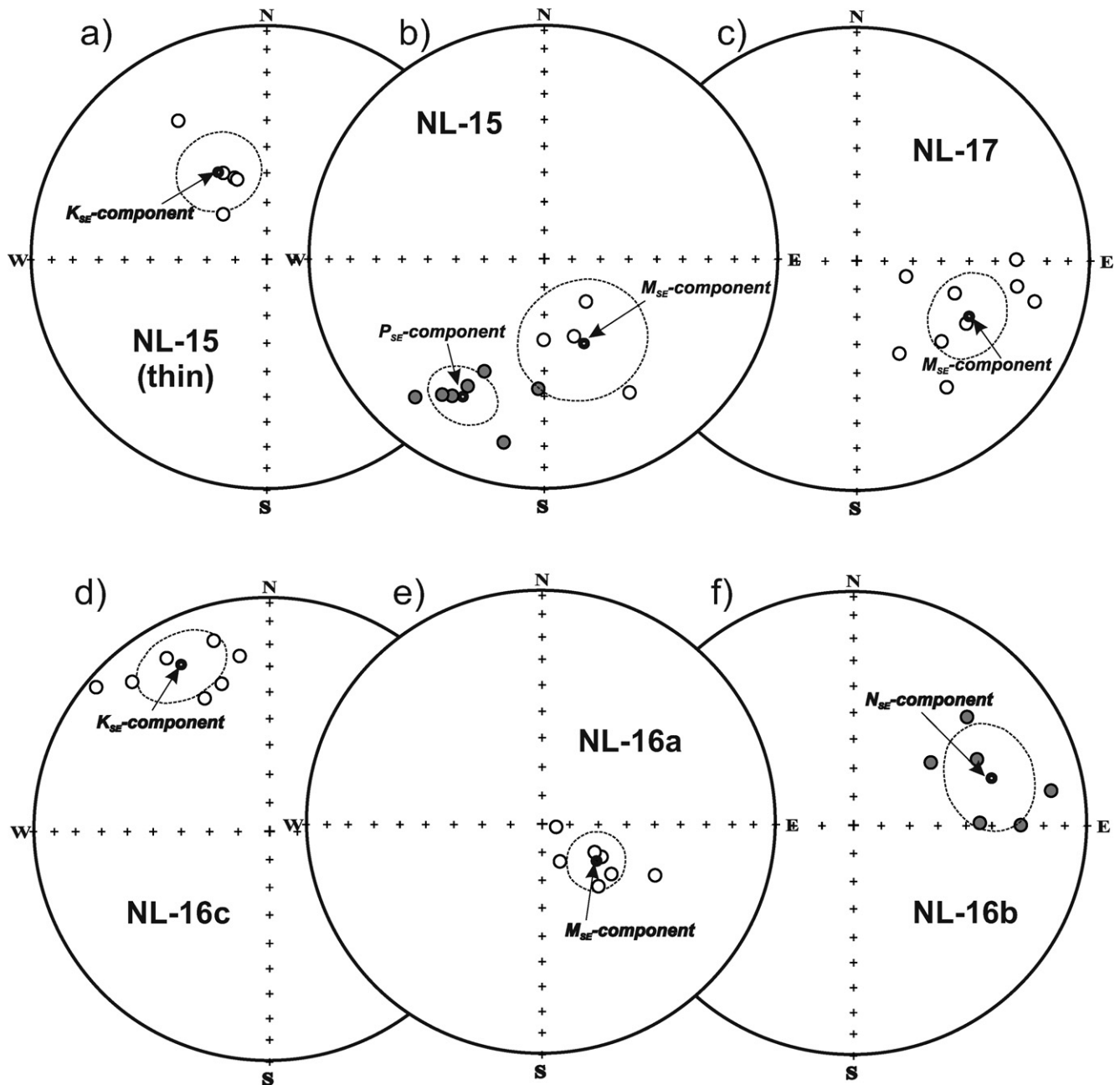


Fig. 10. Sample mean palaeomagnetic directions for the southeastern area. Each site mean direction is shown as a smaller dashed circle with its size given by the α_{95} confidence cone about the mean.

declination and positive inclination (mean direction in Table 1, Fig. 10f).

5.5. Southeasternmost window (SE-, E- and NE-trending dykes)

A total of five sites were sampled in the southeasternmost window (NL-11, -12, -13a, -13b and -14; Figs. 1e and 2a). Three dykes cross-cut each other at NL-13 (Fig. 2a), and one of these belongs to the E-trending swarm of possible similar 2.65 Ga age as the E-trending Rykoppies swarm (see Klausen et al., 2010 for further discussion). One SE-trending braided dyke at NL-13 is cut by this

E-trending dyke and is thereby most likely an outlier of the 2.95 Ga Badplaas swarm. Another SE-trending regular dyke at NL-13, on the other hand, cuts the E-trending dyke and is therefore more likely to be Jurassic. Another E-trending dyke was sampled at NL-14 (Fig. 1e). Two NE-trending and feldspar-phyric dykes of potential 1.90 Ga ages were also sampled at separate sites (NL-11 and -12; Fig. 1e). A baked-contact test was performed at all sites, as well as a conglomerate test at NL-12.

Apart from an occasional low unblocking temperature present-day field component, two main components of magnetization are present: (1) a medium temperature/coercivity component that

SOUTHEASTERNMOST WINDOW

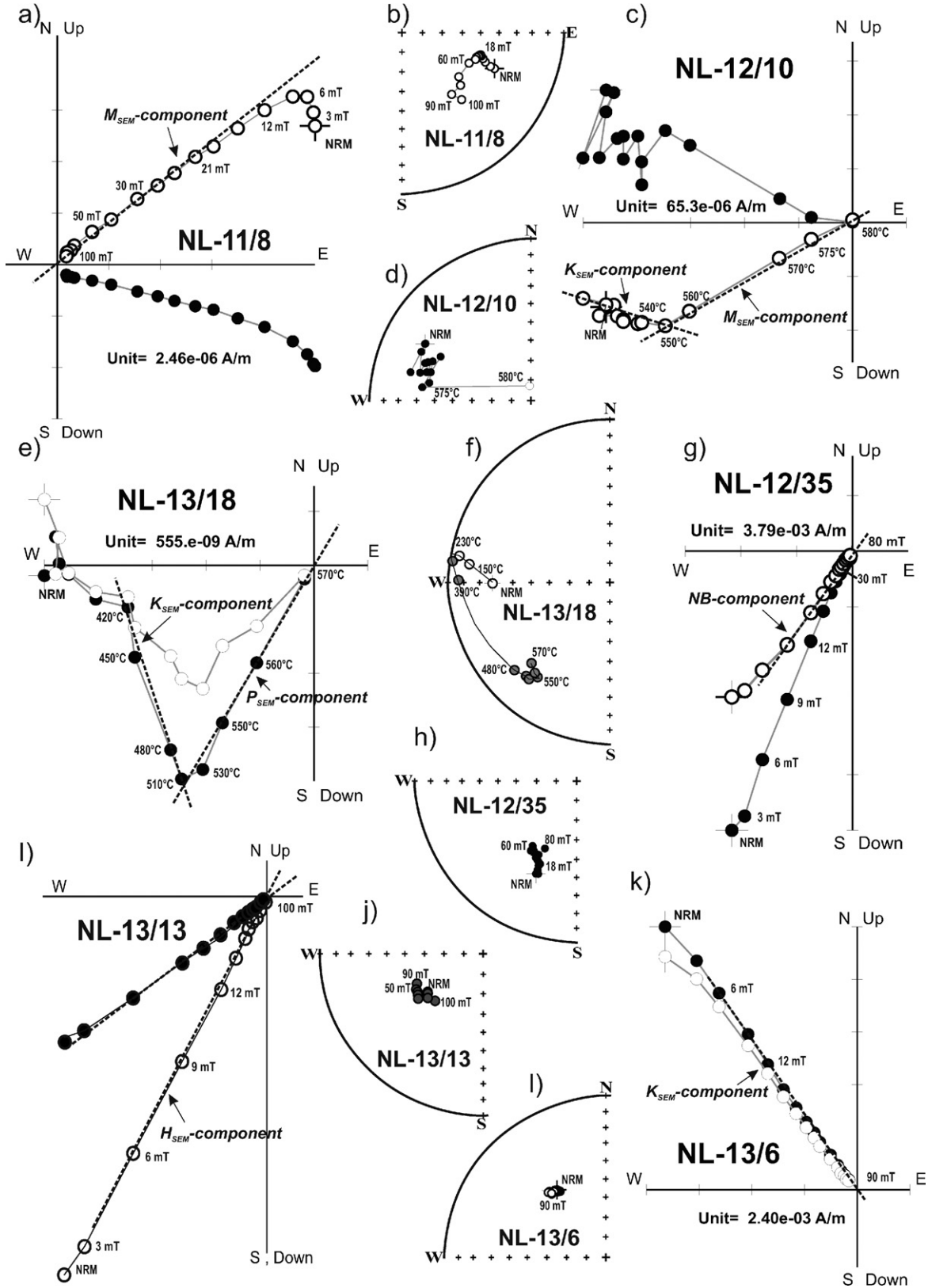


Fig. 11. Examples of thermal and AF demagnetization behavior of specimens from the SE-trending dykes of the southeasternmost area.

SOUTHEASTERNMOST WINDOW

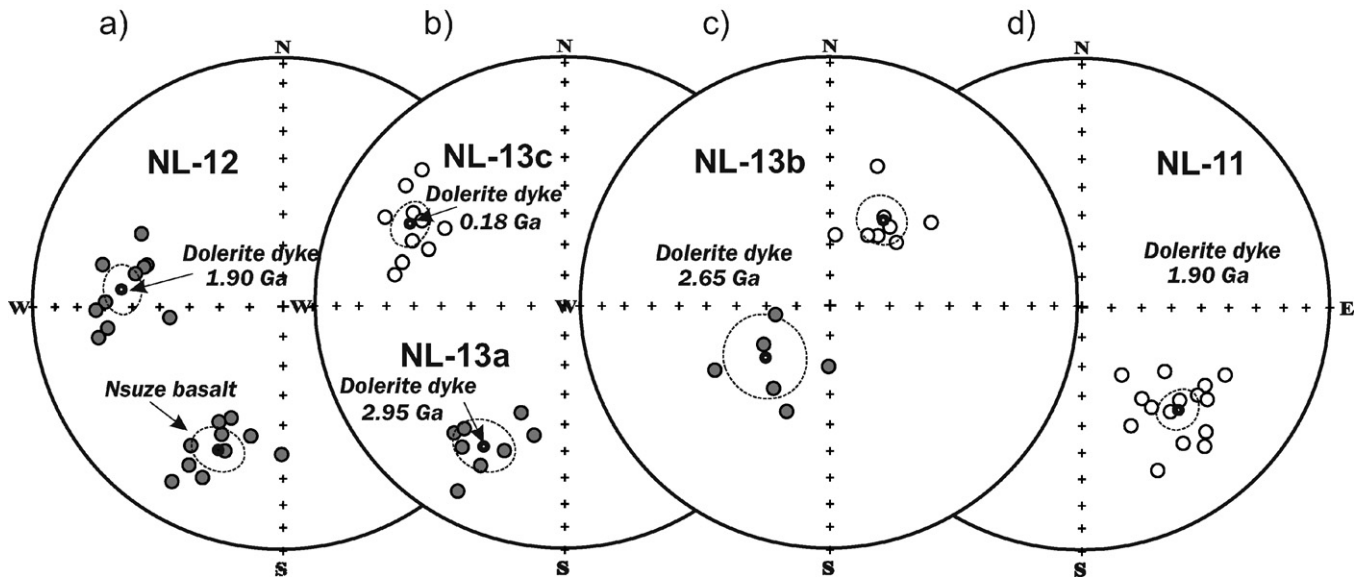


Fig. 12. Sample mean palaeomagnetic directions for the SE-trending dolerite dykes from the southeasternmost area. Each site mean direction is shown as a dashed circle with its size given by the α_{95} confidence cone about the mean.

unblocks between 230 and 450 °C or in alternating fields below 30 mT, and (2) a high temperature/coercivity component that was demagnetized in temperatures up to 540–580 °C and AF fields above 30 mT.

The NE-trending dyke at NL-11 is 10 m wide, contains feldspar phenocrysts and cuts sandstone beds within the Pongola Supergroup. Fourteen samples were collected within the dyke and three from the chilled margin. In addition, samples were collected from the host rock, three from the baked contact, and two from about 200 m away from the dyke margin. A consistent M_{SEM} -component is present in all samples from NL-11 site (Fig. 11a and b). This M_{SEM} -component has a SE-declination and an intermediate-steep negative inclination (Table 1, Fig. 11a and b). The mean direction of this component is given in Table 1 and Fig. 12d.

The NE-trending dyke at NL-12 is 11 m wide (Table 1) and cuts basaltic Nsuze lavas (2980 Ma; Hunter et al., 2006). Stratigraphically beneath the Nsuze lavas are quartzites of the Pongola formation and intraformational conglomerates. Ten samples were collected within the dyke, half from the chilled margin, and half from the dyke center. In addition, samples were collected from the nearby Nsuze lavas, and also from individual pebbles within the conglomerate. The latter samples can be used for a ‘conglomerate test’ to ascertain whether the remnant magnetism was acquired after emplacement of the conglomerate (i.e., a remagnetization) or prior to erosion of the pebbles.

During stepwise thermal and AF demagnetization experiments, two components of NRM were isolated in the majority of specimens from dyke. The first one, K_{SEM} -component of single polarity and is directed to the northwest with steep negative (upwards) inclination. It is isolated in the temperature interval up to 550 °C or in alternating field below 40 mT (e.g., sample NL-12/10, Fig. 11c, d and sample NL-12/11, Fig. 13e). The second remanence direction, M_{SEM} -component has a single polarity which is removed at high temperatures up to 580–590 °C and AF fields above 40 mT (Fig. 11c, d and Fig. 13d, e). This component points to the WNW with positive moderate-shallow inclination (for example, sample NL-12/10, Fig. 11c and d). For the mean directions of this component (see Table 1 and Fig. 12a).

Three dykes at NL-13a, -13b and -14 were sampled within the host Archean basement granitoids (Figs. 1e and 2a). The SE-trending dyke cuts the E-trending, but both are considered to belong to the Badplaas swarm. The two sampled E-trending dykes are located 2 km apart. In addition, samples are collected from a basement-hosted sill of presumed Jurassic age (13c), which cuts the E-trending dyke at NL-14 and probably extended above the dykes at site NL-13. Samples were also collected from Archean basement located to the south for a baked-contact test.

The SE-trending dykes from the presumed 2.95 Ga Badplaas swarm (dyke 13a at Fig. 2a) exhibit two different magnetization components. The first one, K_{SEM} -component has north-western declination and intermediate negative inclination (e.g., NL-13/18, Fig. 11e and f). The second one, P_{SE} -component demonstrates south-southwestern declination and intermediate positive inclination (Fig. 11e and f). The mean direction of this P_{SE} -component for site NL-13a (dyke 13a) is given in Table 1 and Fig. 12b.

A high-temperature H_{SEM} -component characterize the E-trending dykes, which potentially are all members of a very extensive 2.65 Ga Rykoppies swarm (e.g., Klausen et al., 2010). The H_{SEM} -component has south-west declination and steep positive inclination. It is found in samples from dykes 13b and 14 (e.g., sample NL-13/13, Fig. 11j and l). Mean direction of this component is given in Table 1 and Fig. 12c.

Samples NL-13/6 and NL-13/7 taken from the SE-trending regular dyke at site NL-13c and yield a steep NW directed with negative inclination, single stable remanent magnetization component (Fig. 11k, l and Fig. 16a, b). This K_{SEM} -component is isolated in the temperature interval up to 580 °C or in alternating field above 40 mT. Mean direction of K_{SEM} -component (NL-13c) is given in Table 1 and Fig. 16c.

5.5.1. Conglomerate test

Conglomerates from the Pongola Supergroup were collected below R34 road bridge across the White Mfolozi River (Fig. 13c). Ten boulders of various rock types all responded well to demagnetization and two components were readily identified (Fig. 13a). A high temperature/coercivity GF-component is isolated in the

SOUTHEASTERNMOST WINDOW

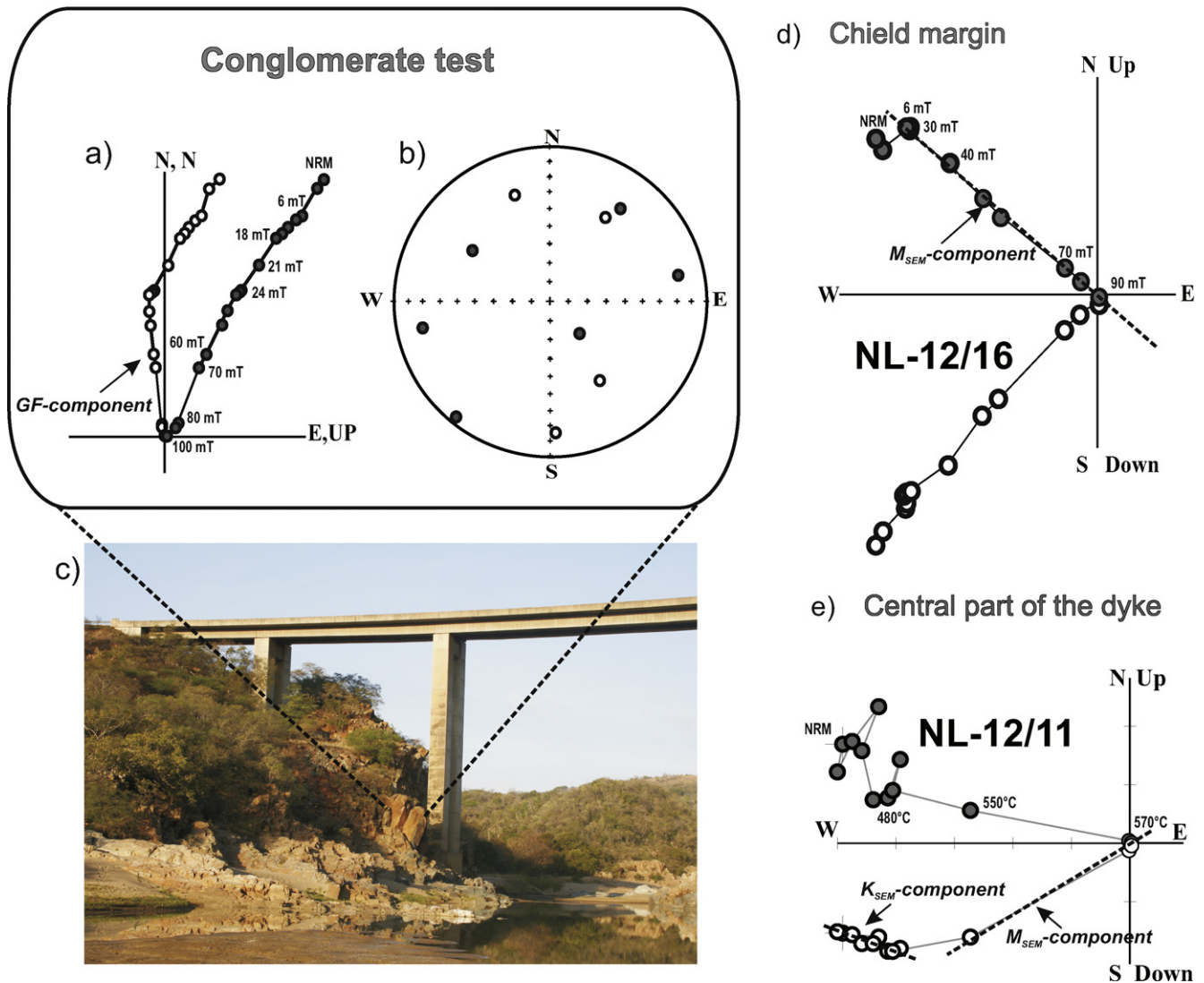


Fig. 13. Results from intraformational conglomerate test at site NL-12 of the southeasternmost area.

temperature interval 450–580 °C or in alternating field 40–100 mT (Fig. 13a). The directions are plotted in Fig. 13b. The test for uniform randomness (Watson, 1956) gives a positive result when applied to these GF-directions. These results imply that the magnetizations preserved in the Nsuzé basalts and cross-cutting dolerite dykes are primary and not a later remagnetization.

5.5.2. Baked-contact test

A baked-contact test was attempted at all three localities (NL-11, NL-12 and NL-13 + 14). At NL-11 and NL-13 + 14 we sampled within the baked-contact zone, and host rock granitoids were collected about 3–5 m from the dykes as well as about 200 m away from the dykes.

The samples of baked granitoids exhibit two components during demagnetization. The low-coercivity or “soft” demonstrate present-day geomagnetic field component. A southeastern upward component then unblocks up to the temperatures of about 560 °C and in AF fields above 40 mT (NL-11/11).

The same two components are readily identified in the samples collected from the chilled margin and dyke (samples NL11/8

and NL-11/2, Fig. 14, respectively). In samples of the unbaked granite-gneisses about 200 m away from the dykes, demagnetization follows a great circle arc trajectory away from negative intermediate south-easterly directions towards a shallow south-western and downward direction, which forms a stable end-point of thermal demagnetization between 420 °C and 560 °C and AF fields above 50 mT (Fig. 14).

Since chemical and/or thermal remagnetization of the host rock is expected to be total at the contact with dykes, we interpret the M_{SEM} -component to be equivalent to the dykes' primary thermo-remanent magnetization.

At site NL-12, where the NE-trending dyke intrudes Nsuzé lavas, samples were collected both within the baked-contact zone and up to 50 m away from the dyke. Samples from the baked-contact zone show a present-day field and M_{SEM} -components (Table 1, Fig. 15).

Samples from unbaked-zone, collected about 50 m away from the dyke, yield a shallow-intermediate SW directed with positive inclination, single stable remanent magnetization component (Fig. 11g, h and Fig. 15). This NB-component is isolated in the tem-

SOUTHEASTERMOST WINDOW CONTACT TEST

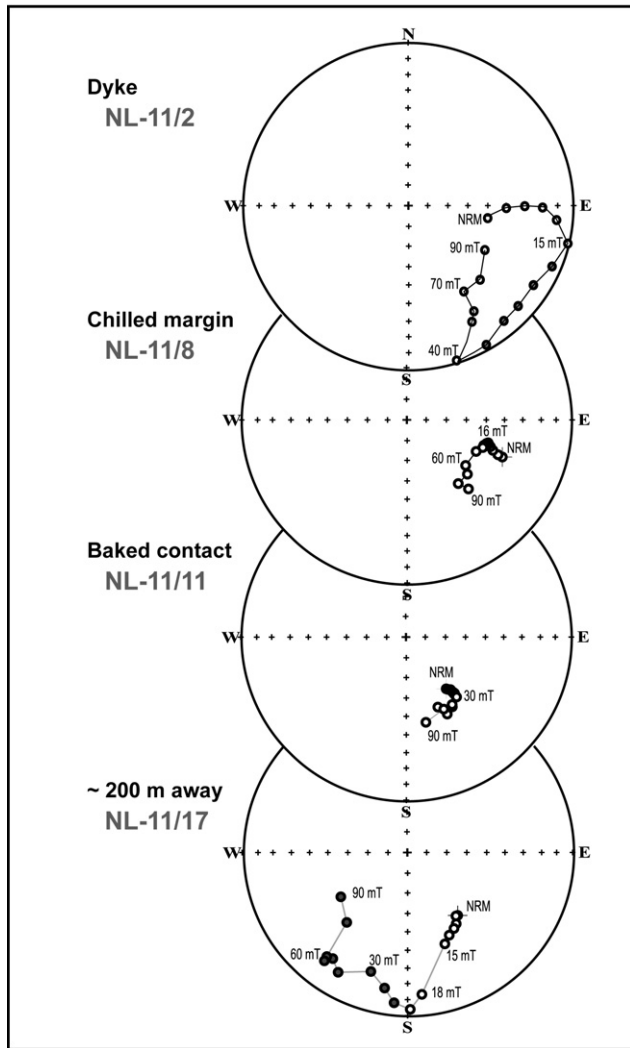


Fig. 14. Paleomagnetic baked-contact test at NL-11 of the southeasternmost area plotted on equal-area stereonets.

perature interval up to 560°C or in alternating field up to 80 mT. Mean direction of NB-component is given in Table 1 and Fig. 12a. Based on positive contact and conglomerate tests we argue for a primary origin of M_{SEM} -component separated in NE-trending dykes.

6. AMS results

The AMS was measured on about 15 samples from each dyke and the results are summarized in Table 2.

6.1. Northeastern area (Black Hills swarm)

The individual site data are presented in Table 2. Data from sites NL-25 to -27 exhibit a range in P (degree of anisotropy) up to 10%, and have T (shape parameter) with mostly negative values indicative of a prolate (lineated) fabric (Fig. 17). The K3 axes are grouped vertically while K1 and K2 axes are broadly distributed within the horizontal plane. This fabric-type has been observed in many dyke

SOUTHEASTERMOST WINDOW CONTACT TEST

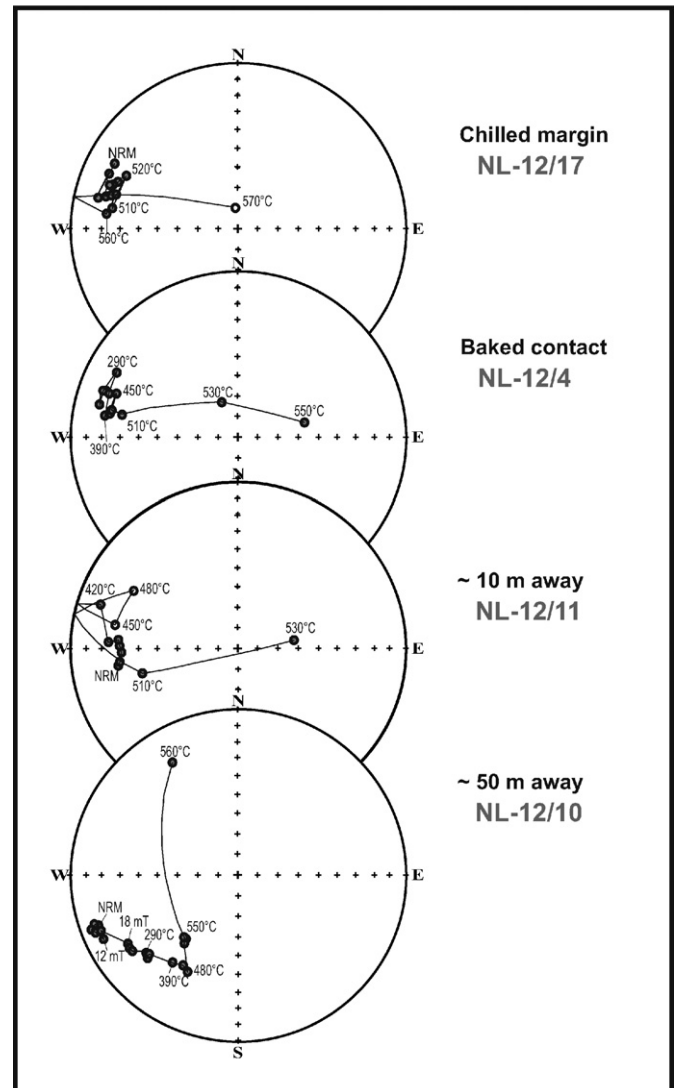


Fig. 15. Geological sketch map of the baked-contact test at SE dyke (NL-12) and Nsuzze basalts and equal-area plots of sample demagnetization progressively farther away from the dyke in the southeasternmost area.

studies (e.g., Park et al., 1988; Ernst and Baragar, 1992) and can be related to post-emplacement processes during cooling that may relate to pure shear type flattening of the column of magma and extension mainly along the dyke trend, resulting a rotation of the minimum axes to vertical. The few available samples from NL-28 give a scattered distribution.

6.2. Eastern area (Rykoppies swarm)

Data from sites NL-21 to -23 exhibit low P (degree of anisotropy) of about 0.5–1%. T (shape parameter) is positive and therefore indicative of an oblate fabric (Fig. 18). The AMS pattern for these sites is clear: K1 is subvertical and K3 is nearly normal to the dyke trend, and this fabric indicates vertical flow. However, it is not clear why the K1 data is oblique to the plane of the dyke by about 30°. At NL-20, the P values approach 1% anisotropy and T

Table 2
AMS data for dolerite dykes from the eastern Kaapvaal Craton.

Site	Strike	N	K_{mean}	S.D.	Max			Int			Min			L	F	P_j	T
					Dec	Inc	Conf. angle	Dec	Inc	Conf. angle	Dec	Inc	Conf. angle				
Black Hills swarm, Northeastern area (NE-trending 1.85 Ga dykes)																	
NL-25	60	7	4.05e–02	2.49e–03	97.0	5.4	59.5/7.3	187.2	2.3	59.5/17.2	299.8	84.1	18.2/4.8	1.005	1.014	1.020	0.460
NL-26	35	7	2.24e–03	3.18e–03	73.8	12.1	43.4/4.0	342.4	6.2	43.5/6.1	225.8	76.3	6.9/3.9	1.005	1.014	1.019	0.520
NL-27	65	9	2.31e–03	1.96e–03	177.0	0.5	35.1/5.1	87.0	5.1	35.6/14.1	273.1	84.9	17.1/7.0	1.027	1.015	1.043	–0.283
NL-28*	57	5	3.19e–02	4.78e–03	57.6	6.7	19.9/5.2	148.8	9.6	14.5/7.9	293.0	78.2	17.0/5.1	1.011	1.010	1.021	0.011
Rykpoppies swarm, eastern area (E-trending 2.65 Ga dykes)																	
NL-20*	117	19	8.14e–04	1.10e–04	257.7	80.4	33.1/15.1	134.9	5.2	34.3/19.5	44.2	8.0	22.2/15.0	1.002	1.003	1.004	0.230
NL-21	90	12	1.50e–03	2.77e–03	316.5	59.6	24.4/9.6	116.4	28.8	22.0/14.8	211.2	8.8	17.6/14.1	1.003	1.006	1.006	0.142
NL-22	90	8	1.24e–03	1.02e–03	268.3	53.6	49.8/7.8	23.5	17.4	74.3/31.7	124.3	30.8	73.6/10.3	1.004	1.000	1.004	–0.772
NL-23	90	6	5.81e–04	2.72e–05	91.6	55.2	84.3/12.2	292.9	32.9	84.3/10.4	196.4	10.0	13.8/10.5	1.000	1.006	1.006	0.976
NL-24*	90	7	5.60e–04	2.39e–05	318.9	80.3	68.2/26.3	85.7	5.8	68.2/25.5	176.5	7.7	29.4/21.9	1.000	1.002	1.003	0.813
Badplaas swarm, southeastern area (NW-trending 2.95 Ga dykes)																	
NL-15	135	19	1.86e–02	2.38e–02	128.0	27.6	35.8/7.5	259.6	51.8	37.2/10.3	24.5	24.3	17.4/6.4	1.016	1.014	1.020	0.413
NL-18	144	12	3.76e–02	1.24e–02	128.6	34.4	38.8/11.0	320.4	55.0	38.7/10.0	222.4	5.6	13.6/6.7	1.005	1.029	1.037	0.680
NL-19	130	7	3.46e–02	2.43e–02	293.3	68.8	21.7/7.9	133.5	20.2	25.9/11.9	41.0	6.8	21.3/3.5	1.012	1.024	1.024	–0.022
Black Hills swarm (?), southeastern area (NE-trending 1.85 Ga? dykes)																	
NL-16	60		3.82e–02		246.2	64.3		35.2	22.4		130.2	11.9		1.015	1.004	1.020	–0.601
NL-17	75	9	4.32e–02	2.14e–02	130.3	34.8	68.1/29.4	262.8	44.2	68.6/31.0	20.7	25.7	40.1/30.3	1.002	1.010	1.013	0.644
Karoo swarm, southeastern area (N-trending 0.18 Ga dykes)																	
NL-15/1	176	6	2.75e–02	2.12e–02	28.9	50.0	48.7/3.9	184.9	37.5	48.7/4.9	323	12.0	5.5/4.7	1.005	1.035	1.044	0.748
Black Hills swarm (?), southeasternmost area (NE-trending 1.85 Ga? dykes)																	
NL-11	50	5	7.41e–04	1.05e–04	53.6	29.8	15.3/6.7	159.3	25.3	15.9/5.2	283.3	49.1	17.3/9.3	1.007	1.004	1.011	–0.231
Badplaas swarm (?), southeasternmost area (NW-trending 2.95 Ga? dykes)																	
NL-13	135	9	7.73e–04	2.34e–04	326.5	10.0	39.9/18.2	128.2	79.4	48.4/33.2	235.9	3.2	45.0/17.9	1.002	1.003	1.006	0.149
Rykpoppies swarm (?), southeasternmost area (E-trending 2.65 Ga? dykes)																	
NL-14	80	8	1.06e–03	1.52e–04	167.4	75.9	18.0/9.8	269.3	2.9	35.0/8.3	360.0	13.7	34.8/17.5	1.013	1.007	1.019	–0.321

Note: * indicates site for which a U–Pb baddeleyite age was determined by Olsson et al. (2010).

SOUTHEASTERNMOST WINDOW “Karoo” remagnetization

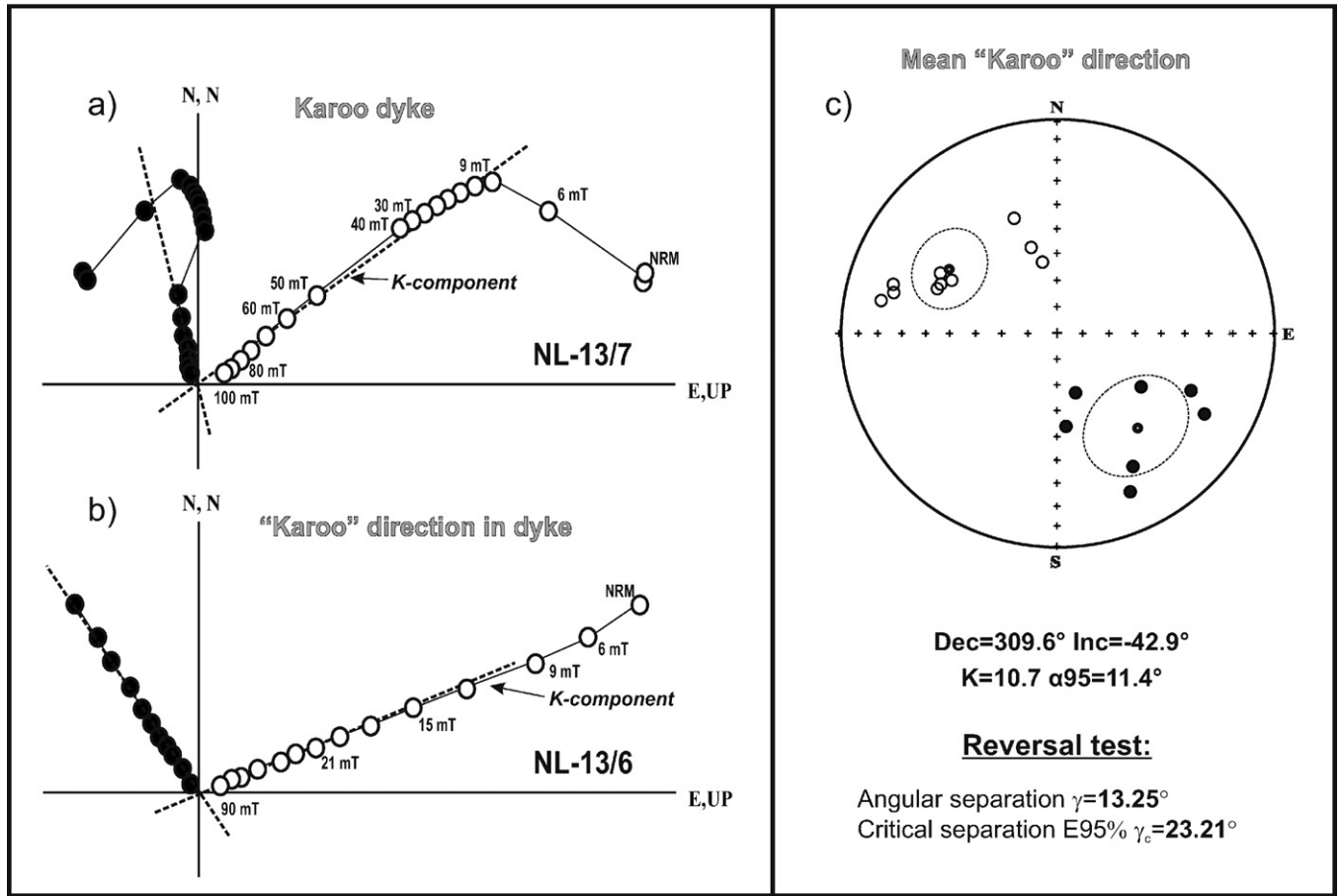


Fig. 16. Results from the ‘Karoo’ dyke (southeasternmost area, site NL13 which trends N135°E) (a) representative sample behavior from the Karoo dyke at site NL13, (b) representative sample behavior with Karoo component site NL13 (dyke trending N80°E) in the southeasternmost area; (c) site mean paleomagnetic directions of the K-components for the dyke swarm of the southeasternmost area. The mean directions are shown as smaller circle. Dashed circles denote cones of α_{95} confidence about the mean.

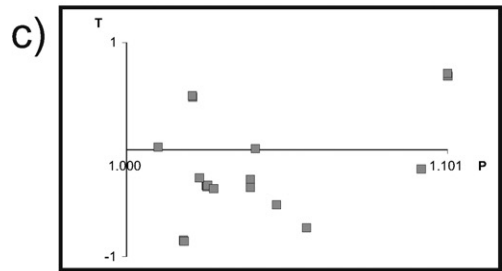
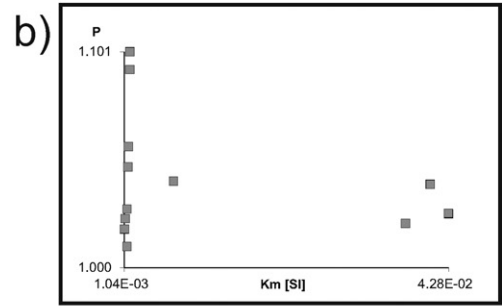
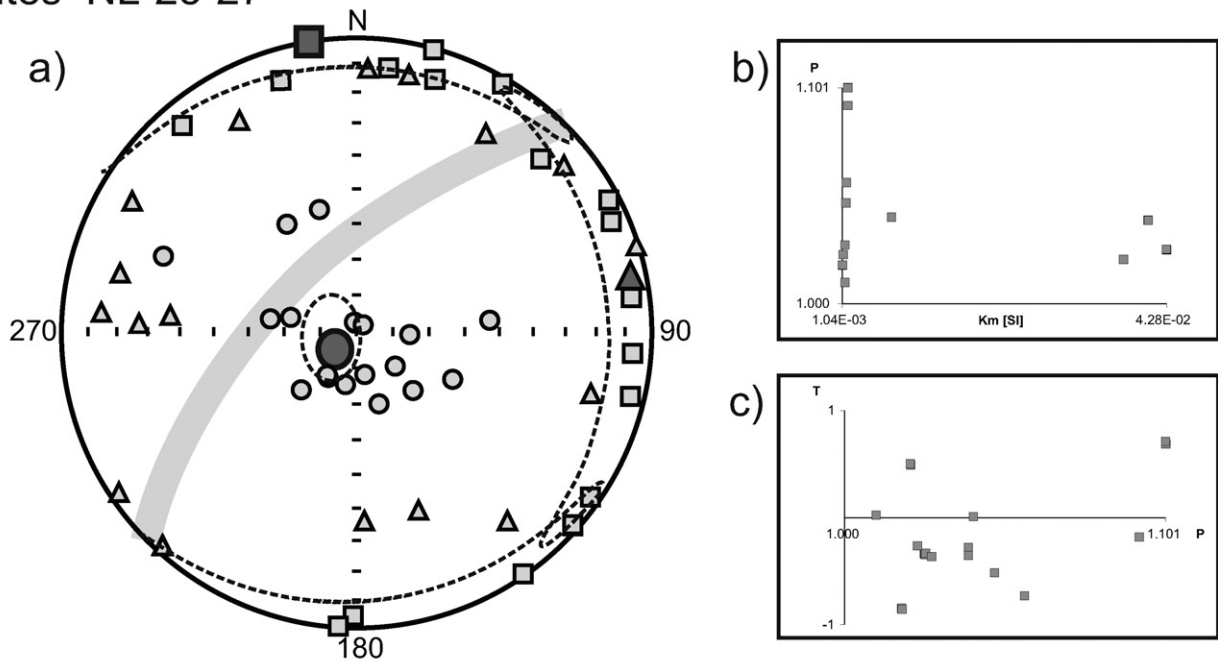
Table 3
Summary of paleomagnetic poles for the Kaapvaal Craton (from published data).

Unit	Label	Paleopole		D_p (°)	D_m (°)	Paleolatitude (°)	Age	Reference
		Latitude (°N)	Longitude (°E)					
Karoo dolerite dykes	KD	-68.3	93.7	7.0	7.0	33.6	183 ± 2 Ma	Hargraves et al. (1997)
Karoo N-trending dykes	KAR	-61.3	125	6.9	11.8	19.1	0.18 Ga	This study
Namaqua overprint	NM	50.6	19.6	9.9	9.9		1244 ± 30 Ma	Evans et al. (2002)
Post-Waterberg dolerite	PWD	8.6	15.4	17.3	17.3		1875.5 ± 3.5 Ma	Hanson et al. (2004)
Black Hills (NE-trending) dolerite dykes	BHD	9.4	352.0	4.3	5.8	39.4	1.90 Ga	This study
Bushveld complex	BC	-39.5	227.0	10.9		22.8	2050 ± 12 Ma	Hattingh, 1986
Gamara/Mapedi fm.	GM	2.2	81.9	7.2	11.5		2130 ± 92 Ma	Evans et al. (2002)
Southeastern area, N-component	NSA	5.9	93.4	12.0	20.4	21.1	~2.15 Ga	This study
Ongeluk fm	ONG	-0.5	100.7	5.3	5.3	10.9	2222 ± 13 Ma	Evans et al. (1997)
Mbambane pluton	MP	19.7	105.7	9.4	9.4	4.5	2687 ± 6 Ma	Layer (1986), Layer et al. (1989)
Rykoppies (E-trending) dolerite dykes	RYD	-62.1	336.0	3.5	4.2	38.0	2.65 Ga	This study
Allanridge fm	ALF	-67.6	355.8	6.1	6.1		~2.7 Ga	de Kock (2007)
Westonaria basalt	WE	-17.1	47.9	18.8	18.8	68.9	2714 ± 8 Ma	Strik et al. (2007)
Derdepoort basalt	DB	-39.6	4.7	17.5	17.5	64.5	2782 ± 5 Ma	Wingate (1998)
Ushushwana complex	USH	9.2	347.0	7.6	7.6	33.3	2875 ± 40 Ma	Layer (1986), Layer et al. (1988a)
Badplaas (NW-trending) dolerite dykes	BAD	-63.6	285.4	2.3	4.0	18.5	2.95 Ga	This study
Nsuze basalt	NB	-67.0	285.6	5.3	9.2	20.0	2.95 Ga	This study
Nelshoogte pluton	NP	17.6	309.8	9.0	9.0	3.5	3197 ± 18 Ma	Layer (1986), Layer et al. (1998)

Note: D_p , D_m , semi-axes of the cone of 95% confidence about the pole.

NORTHEASTERN AREA

Sites NL-25-27



Site NL-28

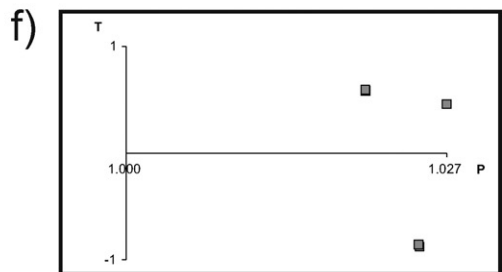
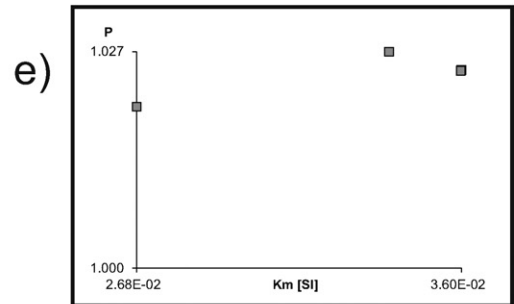
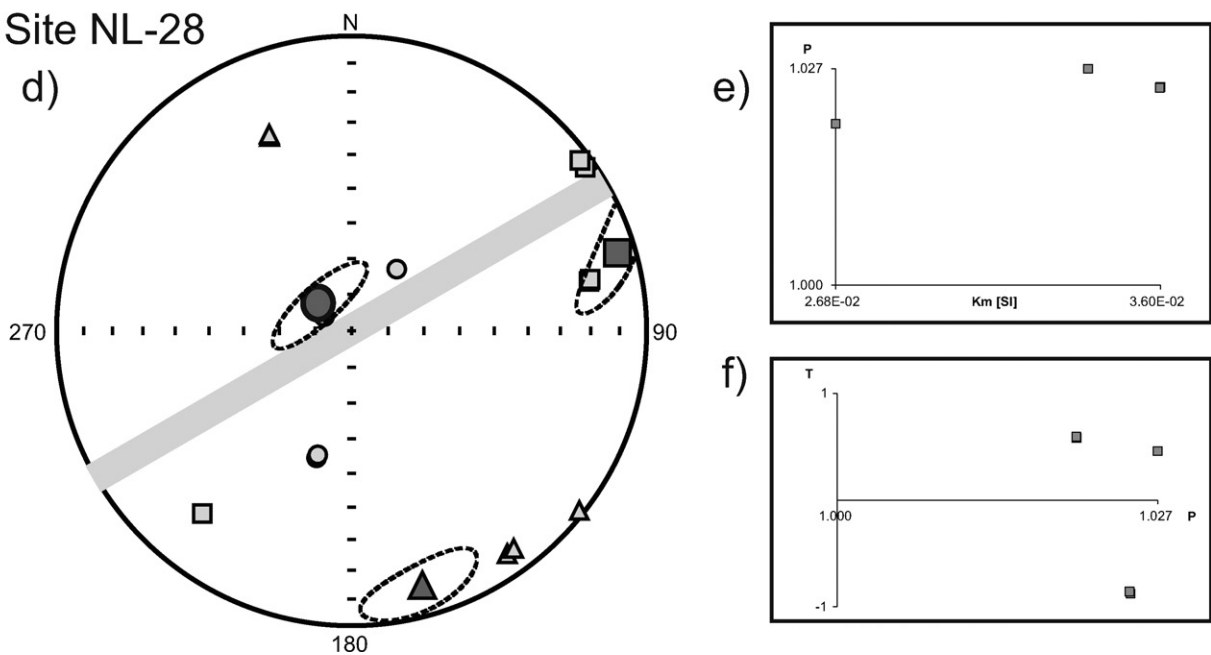


Fig. 17. AMS data for sites NL-25-28 of the northeastern area. T is the shape anisotropy parameter with positive (negative) values indicating oblate (prolate) values. P is degree of anisotropy. AMS directional data plotted on equal-area stereonet: squares give direction of maximum axes, triangles locate intermediate axes, and circles indicate minimum axes. Mean values are given by larger symbols in this and also in Figs. 18–21. Symbols plotted on lower hemisphere. Grey band marks trace of dyke on lower hemisphere. Dashed circles indicate 95% uncertainty.

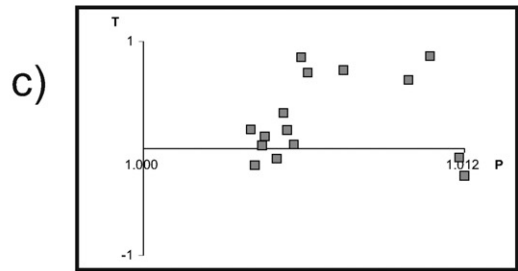
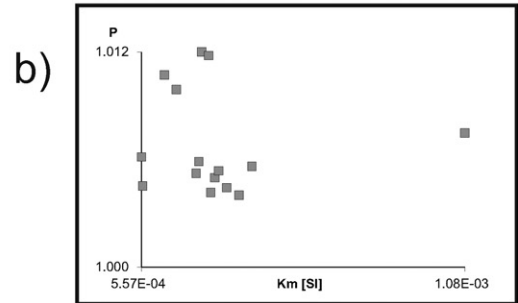
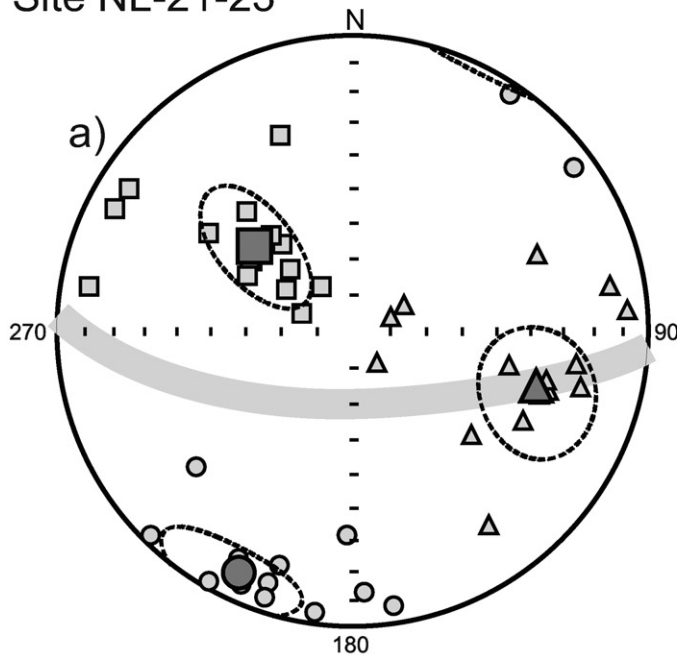
(shape parameter) data straddles the boundary between oblate and prolate fabrics. At site NL-20 the K3 values are perpendicular to the dyke and the maximum axes (K1) are steep, suggesting vertical flow at this site also. Thus data from both the E-trending dykes (sites NL-21 to -23) and also the SE-trending dyke (site NL-20) of the same radiating Rykoppies swarm indicate vertical flow emplacement.

6.3. Southeastern area (SE- and NE-trending dyke swarm)

At site NL-15 there are two dykes. For the data from the contact zone of this site, the degree of anisotropy (P) approaches 2%, and the shape parameter (T) indicate an oblate (foliated) fabric (Fig. 19). The directional data (see the stereonet) indicate a very good vertical flow fabric. For the data from the central part of this main dyke, the

EASTERN AREA

Site NL-21-23



Site NL-20

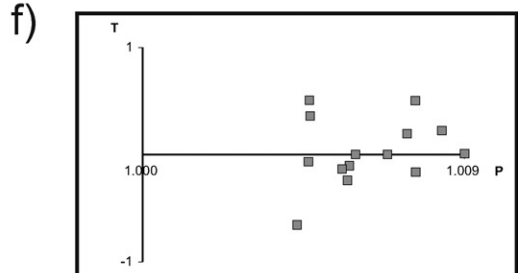
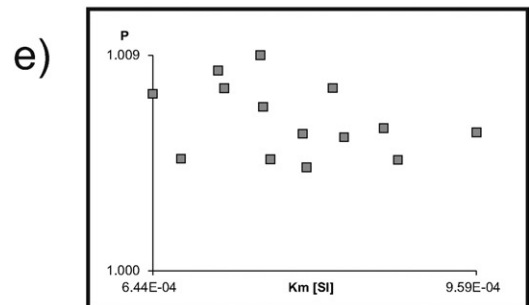
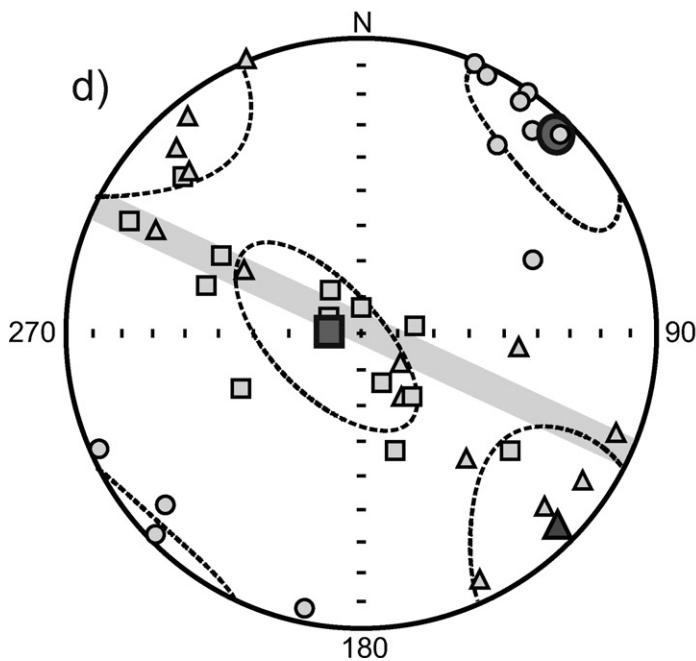


Fig. 18. AMS data for sites NL-20 and NL-21 of the eastern area. Symbols and grey band explained in caption to Fig. 17.

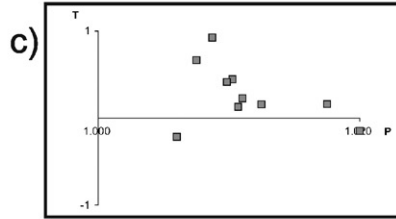
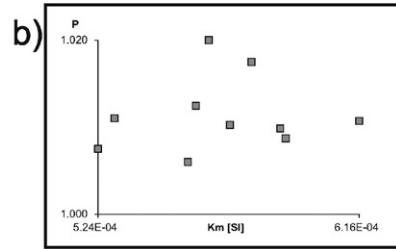
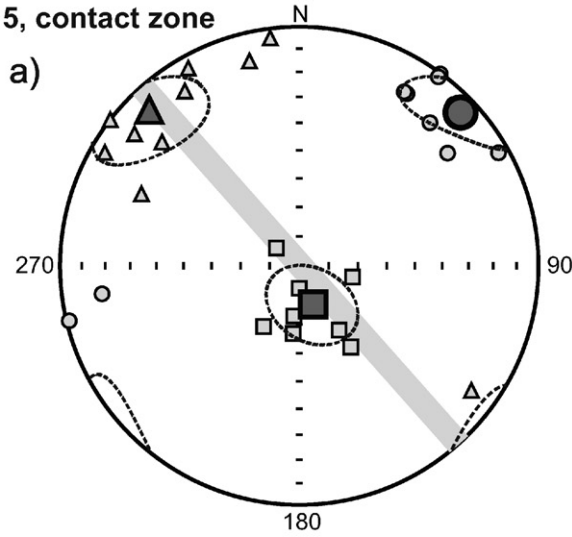
degree of anisotropy is about 4% and the shape factor (T) is both oblate and prolate. The direction data for the central part of the main dyke indicates a horizontal flow fabric. For the data from the other, thin, dyke the degree of anisotropy ranges up to 10% and the shape parameter (T) is oblate but the directions are scattered.

Data from two additional sites, NL-18 and NL-19 (Fig. 20) are presented. At NL-18 the degree of anisotropy (P) is almost 8% and values of the shape factor (T) are mostly oblate. The minimum axes

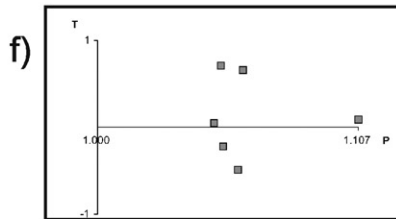
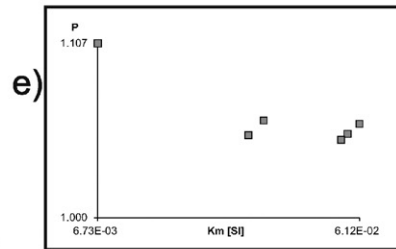
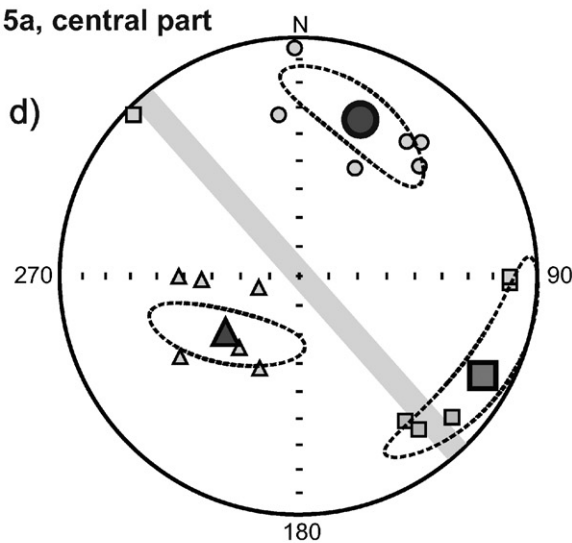
are normal to the dyke and the most of the maximum axes are horizontal in the plane of the dyke suggesting horizontal flow, while a few samples with the steep maximum axes, indicate vertical flow. At site NL-19, the degree of anisotropy is almost up to 8% and the fabric ranges from oblate to prolate. The minimum axes are roughly orthogonal to the dyke and the maximum axes cluster at sleep-intermediate inclinations in the NW quadrant. This pattern is more suggestive of steep flow.

SOUTHEASTERN AREA

Site NL-15, contact zone



Site NL-15a, central part



Site NL-15b, thin dyke NL-15b

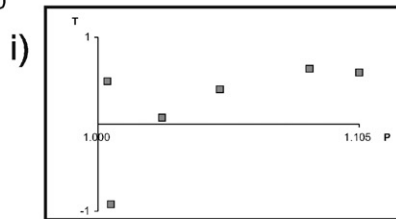
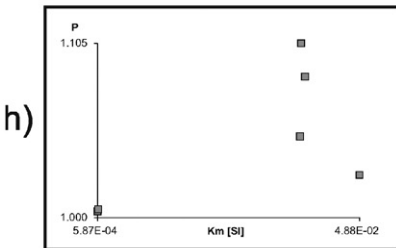
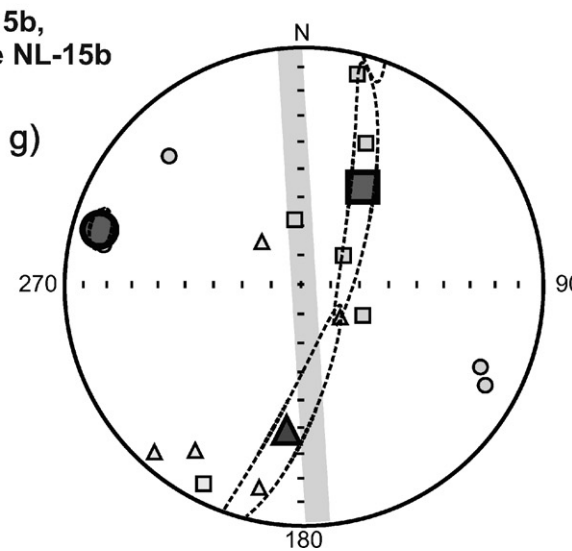
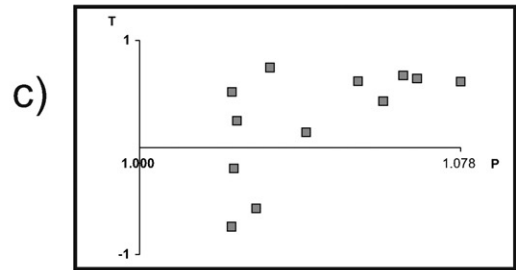
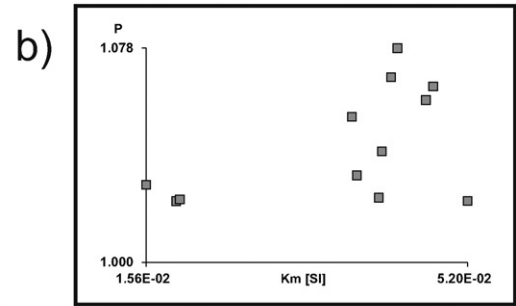
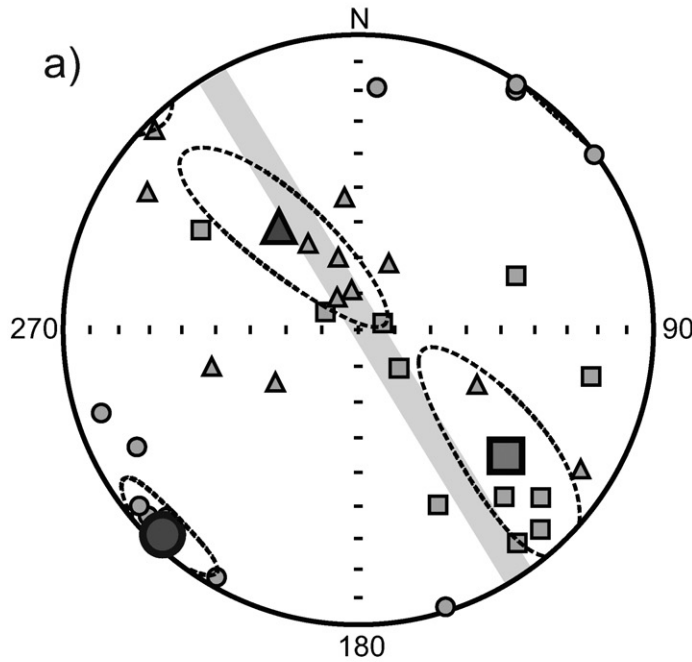


Fig. 19. AMS data from site NL-15 of the southeastern area. “Contact zone” and “central part” are from the margin and interior, respectively of a single thick dyke. “Thin dyke” is from a separate thinner dyke at this site. Symbols and grey band explained in caption to Fig. 17.

SOUTHEASTERN AREA

Site NL-18



Site NL-19

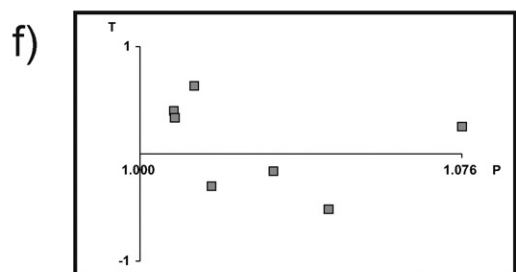
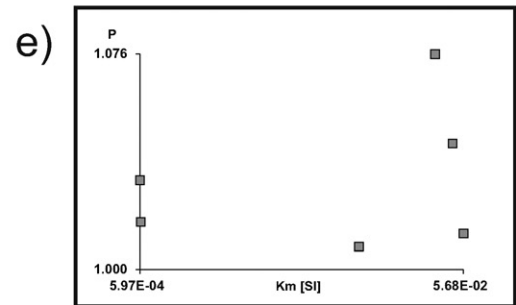
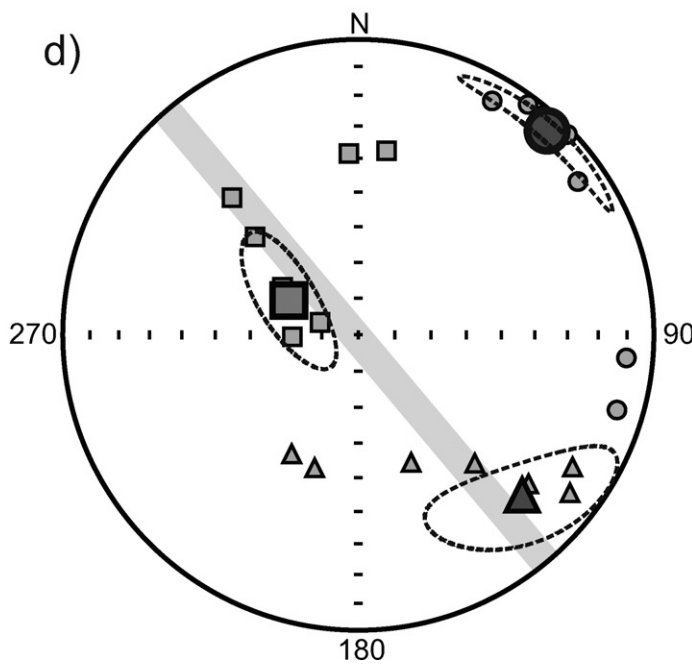


Fig. 20. AMS data from sites NL18 and NL19 of the southeastern area. Symbols and grey band explained in caption to Fig. 17.

6.4. Southeasternmost window (SE-, E- and NE-trending dykes)

The bulk susceptibility and type of anisotropy of magnetic susceptibility of this southeasternmost region (northern KwaZulu-Natal province) are divided into two groups based on dyke thickness and/or age. The first group is composed of samples from thin (<3–5 m) dykes and from the contact zones of thick dykes. As

an example in Fig. 21, two dykes were sampled at NL-13 (Fig. 2a), and thin and a thick dyke of similar trends (Fig. 21). Both dykes have *P* values (degree of anisotropy) up to 2% and an oblate fabric ($T > 1$). The thin dyke exhibits vertical flow (minimum axes perpendicular to the dyke plane) and maximum axes vertical. The thick dyke has a pattern favoring horizontal flow (minimum axes horizontal and maximum axes horizontal).

SOUTHEASTERNMOST WINDOW

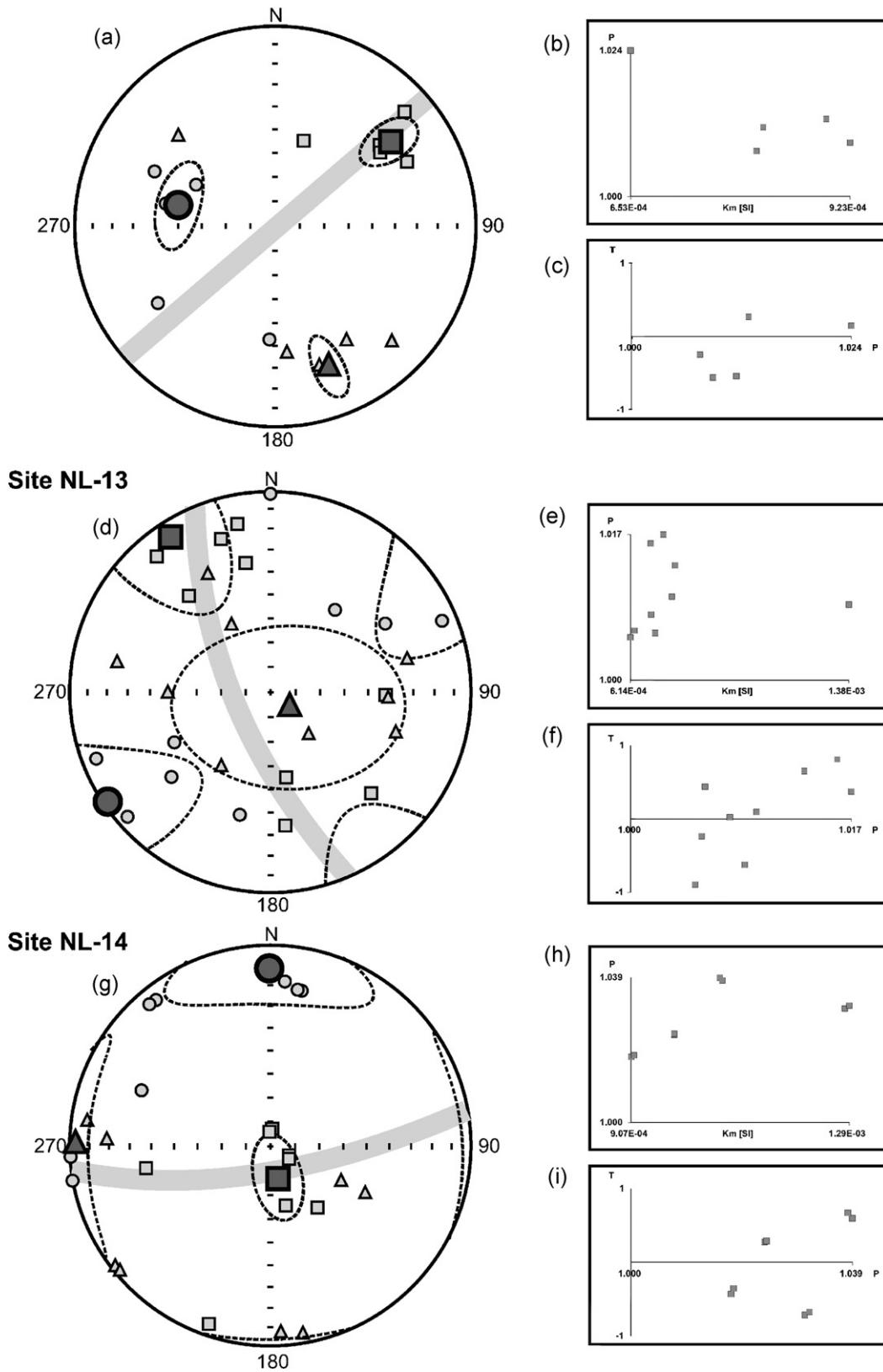


Fig. 21. AMS data from site NL13 of the southeasternmost area. Symbols and grey band explained in caption to Fig. 17.

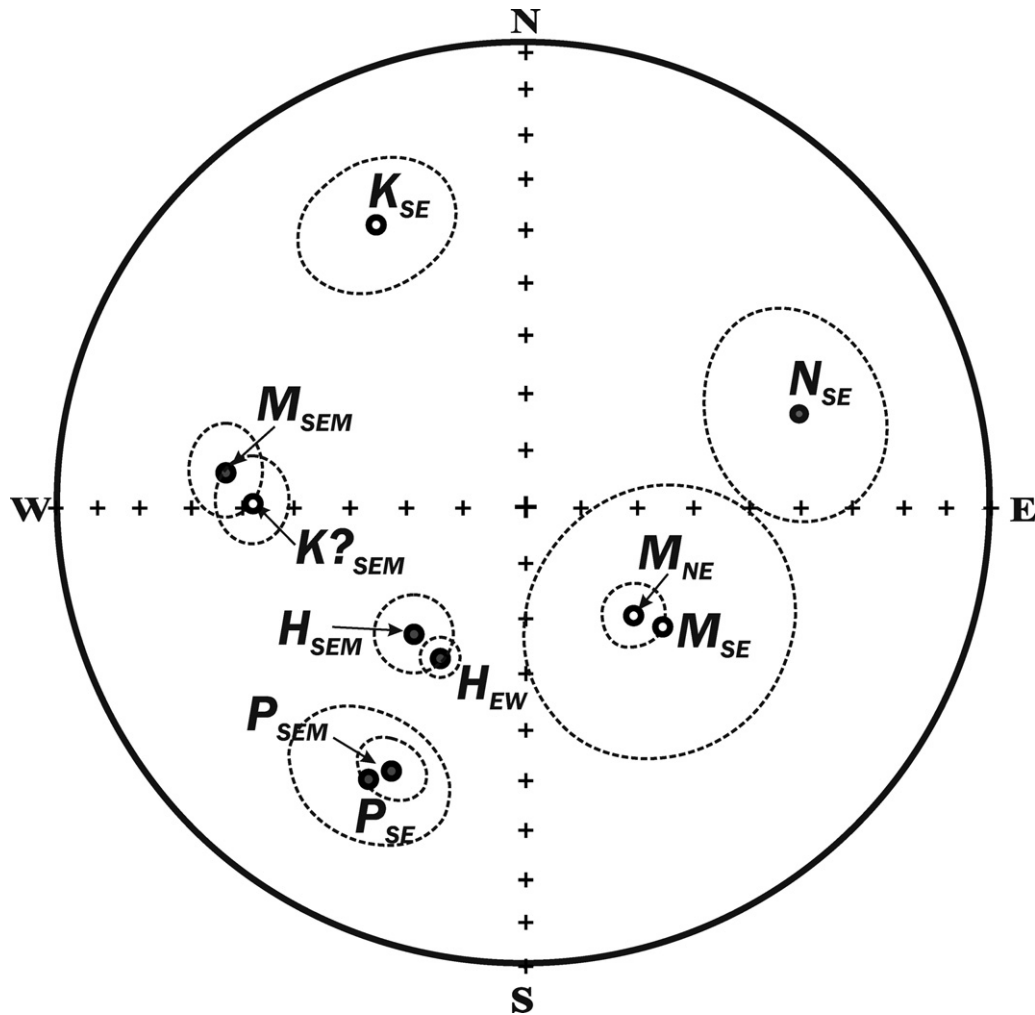


Fig. 22. Paleomagnetic directions from units studied herein plotted on equal-area stereonet on the lower hemisphere. Abbreviations explained in Table 1. Dashed circles show α_{95} cone of confidence about a mean direction.

7. Discussion

As a result of paleomagnetic investigations of dyke swarms in the Kaapvaal Craton five different components have been recognized. Their mean directions are summarized in Table 1.

The first component, named *P*, is identified in dykes of SE trend in the southeastern and southeasternmost areas (P_{SE} and P_{SEM} in Fig. 22). The primary origin of this component is supported by a positive contact test. Therefore we conclude that the 2.95 Ga age of these dykes applies also to the age of their magnetization. A paleomagnetic pole, recalculated from this component (BAD in Table 3 and Fig. 23), is located in high southern latitudes. This direction is similar to that obtained for the 2.95 Ga Nsuze basalts (NB, Figs. 22 and 23; the age of those is 2.95 Ga). These 2.95 Ga poles are about 65° to the west from the 2.7 Ga pole obtained on the Allandridge Formation by Strik et al. (2007).

The second dual polarity *H*-component is characterized for east-trending Rykoppies dykes of southeastern and eastern areas (H_{SEM} and H_{EW} , Fig. 22). The primary origin of these components is supported by positive contact test. As the age of the dyke is 2.65 Ga, this is also the age of magnetization. The paleomagnetic pole (RYD-pole in Table 3 and Fig. 23), recalculated from these components does not correspond to the previously obtained Archean–Paleoproterozoic paleopoles for the Kaapvaal Craton. However, RYD-paleopole, calculated from ‘*H*’ component, is close to the 2.7 Ga pole for Allandridge Formation (Strik et al., 2007; de Kock et al., 2009). However, the

Rykoppies direction is about 20° from the Mbabane pluton (Layer et al., 1998) dated at 2690 Ma (U–Pb, Ar–Ar; Layer et al., 1989). The 2782 ± 5 Ma (SHRIMP U–Pb zircon) Derdepoort volcanics have a similar direction (Wingate, 1998).

The third component (*M*) was found in NE-trending Black Hills dykes from the northeastern, southeastern and southeasternmost areas (M_{NE} and M_{SE} , Fig. 22). This component has a southeast pointing shallow upward directed direction. Mean directions of these components are shown in Fig. 22 and Table 1. A paleomagnetic pole, recalculated from this component (BHD, Fig. 23 and Table 3), matches the pole of 1880 Ma Post-Waterberg dolerites (Evans et al., 1997) and also the 2875 Ma Ushuswana complex (Layer et al., 1988). As the age of the dyke at site NL-28 according to Olsson in Söderlund et al. (2010) is 1.90 Ga, and as the primary origin of magnetization in these dykes are supported by positive contact-, conglomerate- (site NL-12) and reversal tests, we conclude that the age of magnetization is 1.90 Ga (Fig. 23).

The fourth component (*K*) is characteristic of SE-trending dykes in the southeastern area and dykelets and sills in the southeasternmost area (Fig. 22). It is also present as a low-temperature component in southeasternmost and southeastern areas (Table 1). The mean direction of this component for each site is shown in Table 1 and Fig. 22. A paleomagnetic pole KAR, recalculated from this component (Fig. 23, Table 3), is close to the 0.18 Ga pole for a Karoo Dolerite (Hargraves et al., 1997).

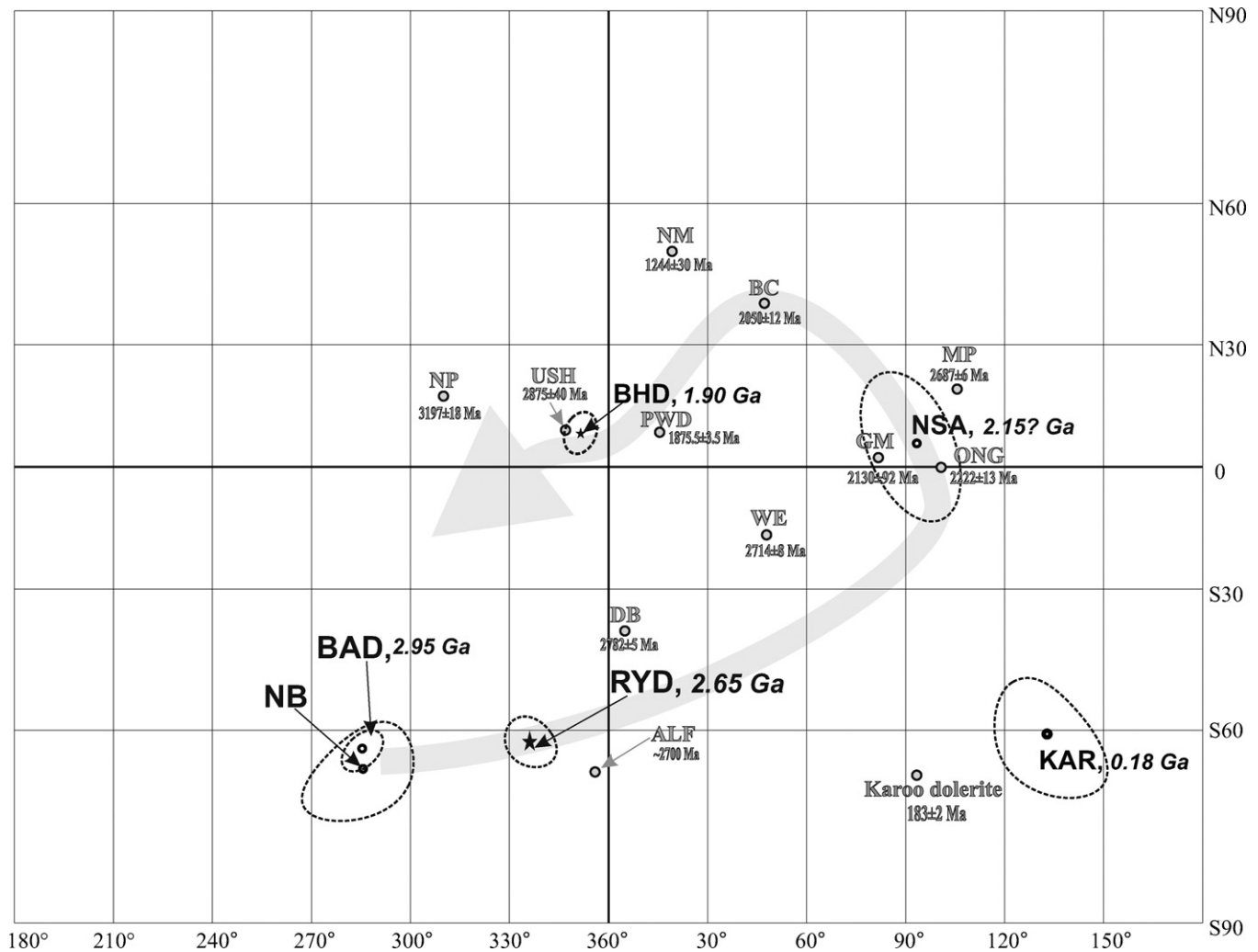


Fig. 23. Paleomagnetic pole positions from units studied herein and compared with reference pole positions from the literature. See summary in Table 3.

The fifth component (*N*) has north–northeastern declination and positive inclination. It is found in dykes of the southeastern area E-trending (NL-16b) dykes. This paleomagnetic pole (NSA in Fig. 23 and Table 3) is close to the pole of Ongeluk Formation with an age of 2.22 Ga (Evans et al., 1997) and the Gamagara Formation with an age of 2.13 Ga (Evans et al., 2002).

As discussed above and summarized in Tables 1 and 3 we have obtained paleomagnetic poles for each of the swarms. We have also demonstrated that each pole position is primary based on a successful baked contact for each swarm, a reversal test for the 2.65 Ga Rykoppies swarm, and conglomerate test for the 1.90 Ga Black Hill swarm. In addition, we distinguished overprint directions that can be related to thermal effects of a nearby sill, whose Karoo age was confirmed by determining its paleomagnetic direction.

AMS data from the 1.90 Ga NE-trending Black Hills dykes (Fig. 17) do not exhibit a clear flow fabric but instead show evidence of a ‘compaction’ fabric acquired after the magma stopped moving (e.g., Park et al., 1988). In contrast, the dykes of the Rykoppies swarm (NL-20 to -23) consistently indicate vertical flow (Fig. 18). From the Ernst and Baragar (1992) AMS study of the Mackenzie radiating swarm of northern Canada, it was inferred that vertical emplacement of dykes was restricted to within about 500 km of the plume center (marked by the focus of the radiating swarm) and that horizontal emplacement occurred at greater distances from the plume center. The vertical flow in sites NL-20 to -23 of the

Rykoppies swarm is consistent with the less than 100 km distance of these sites from the possible plume center based on convergence of dyke trends from sites NL-21 to -23 (E–W trends) and NL-20 (NW-trend).

For the sites in the southeastern region (all from the Badplaas swarm) the AMS patterns are not uniform (Figs. 19 and 20). At site 15 in the southeastern region, a NW-trending dyke exhibits an initial vertical flow fabric (recorded in near margin samples) and a later horizontal flow fabric (recorded in samples collected from the interior of this dyke). In the southeastern area, at site NL-18 (Fig. 20a–c) both horizontal and vertical flow fabrics are preserved. For site NL-19 (Fig. 20d–f) a steep flow fabric is suggested. From the southeastermost area, the thin dyke at site NL-13 exhibits vertical flow while the thick dyke exhibits dominantly horizontal flow.

Our paleomagnetic drift plot (Fig. 24) illustrates the variation in paleolatitude and orientation of the Kaapvaal through late Archean and Paleoproterozoic time based on the data herein (four new determinations) and also from published sources (three poles). Specifically, from 2.95 Ga, through 2.78 Ga and 2.65 Ga the orientation of the Kaapvaal Craton seems to have remained constant, and in fact similar to the present-day orientation. However, the paleolatitude changes significantly, moving from near the equator at 2.95 Ga, southward to $>60^\circ$ S at 2.78 Ga and again northward to about 40° S at 2.65 Ga. Between 2.65 Ga and 2.22 Ga the Kaapvaal

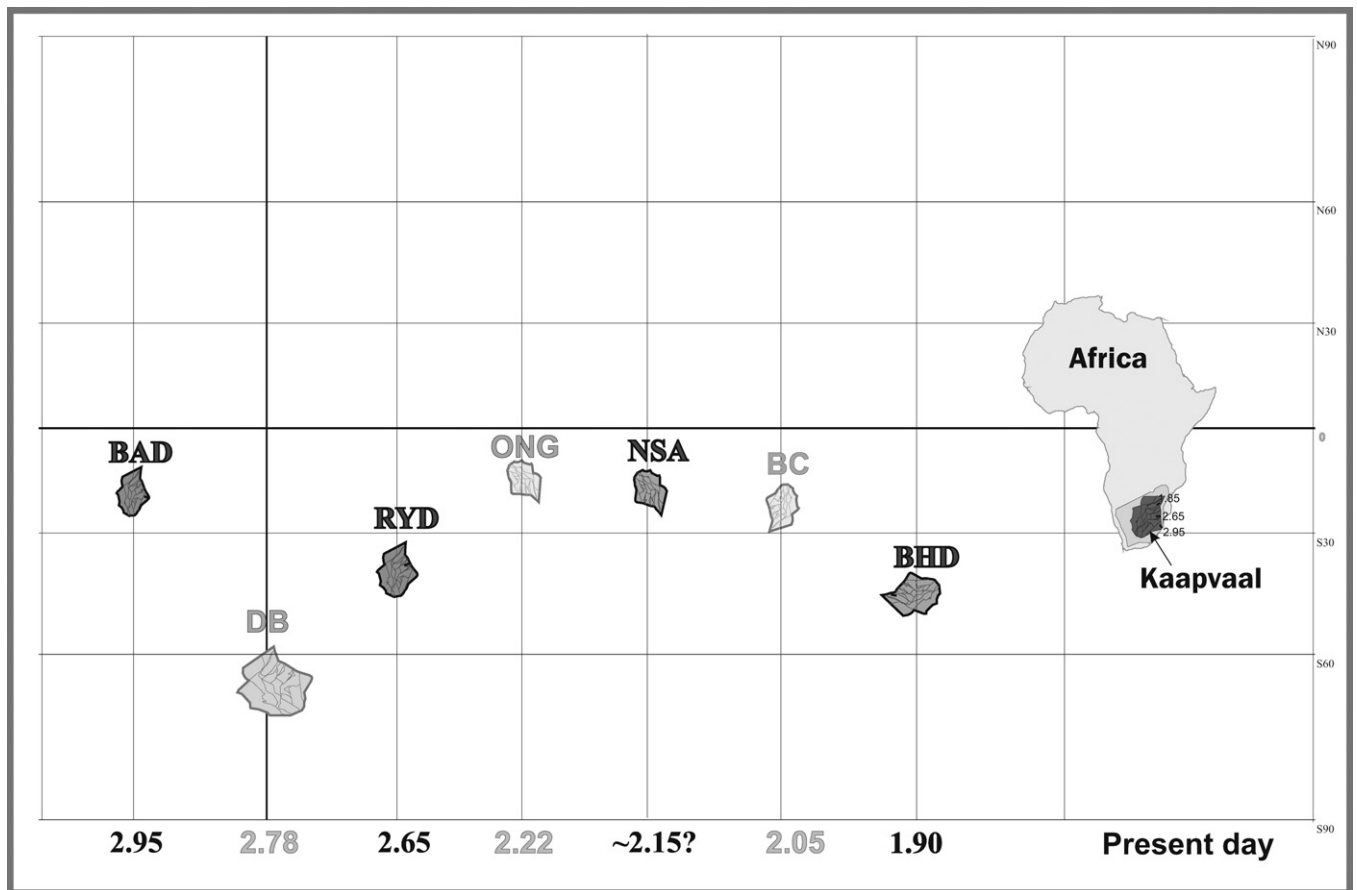


Fig. 24. Latitudinal drift and rotation diagram (cf. for the Kaapvaal Craton based on four poles from this study and three published poles (DB – Derdepoort from Wingate, 1998; ONG – Ongeluk lavas from Evans et al., 1997; and BC – Bushveld Complex from Hattingh, 1986). More details are in Fig. 23 and Tables 1 and 3. In general, because of the polarity ambiguity in the paleomagnetic data, the Kaapvaal Craton could be rotated and placed antipodally (in the opposite hemisphere). However, for simplicity only one polarity option is shown.

Craton changed modestly in paleolatitude (moving slightly northward) but rotated dramatically (by about 140° clockwise). Between 2.22 and ca. 2.15 Ga the position and orientation remained constant giving us more confidence that the data for both 2.22–2.15 Ga are reliable. Through to 2.05 Ga (Bushveld Complex time) the latitude remained constant and there is a slight further clockwise rotation of the Kaapvaal Craton (about 40°). Our remaining key pole occurs at 1.90 Ga by which time the paleolatitude increased slightly (to the south, reaching about 45° S), and there is still a further 80° clockwise rotation. Of course there is a polarity ambiguity for each value and therefore, it cannot be excluded that during some of these intervals the Kaapvaal Craton was in the antipodal position (i.e., in the northern hemisphere and rotated by 180°). As the APWP is developed for other cratonic blocks, this pattern for the Kaapvaal Craton can be usefully compared in order to constrain NeoArchean–Paleoproterozoic reconstructions involving the Kaapvaal Craton.

Acknowledgments

We are indebted to Roman Dorofeev for his participation in the fieldwork. Technical support for field work and sample preparation from the School of Geosciences, University of KwaZulu-Natal is appreciated. NL acknowledges RFBR, project 07-05-01140. We also thank Johan Olsson for discussions and a review of the paper. We thank journal reviewers Pat Eriksson and Michael T.D. Wingate for thorough and helpful reviews.

References

- Anhaeusser, C.R., 2006. Ultramafic and mafic intrusions of the Kaapvaal Craton. In: Johnson, M.R., Anhaeusser, C.R., Thomas, R.J. (Eds.), *The Geology of South Africa*. Geological Society of South Africa/Council for Geoscience, Johannesburg/Pretoria, pp. 95–134.
- Aspler, L.B., Chiarenzelli, J.R., 1998. Two Neoproterozoic supercontinents? Evidence from the Paleoproterozoic. *Sedimentary Geology* 120 (1–4), 75–104.
- Barker, O.B., Brandl, G., Callaghan, C.C., Callaghan, P.G., Eriksson, P.G., van der Neut, M., 2006. The Soutpansberg and Waterberg Groups and the Nlouberg formation. In: Johnson, M.R., Anhaeusser, C.R., Thomas, R.J. (Eds.), *The Geology of South Africa*. Geological Society of South Africa/Council for Geoscience, Johannesburg/Pretoria, pp. 301–318.
- Brandl, G., Cloete, M., Anhaeusser, C.R., 2006. Archaean greenstone belts. In: Johnson, M.R., Anhaeusser, C.R., Thomas, R.J. (Eds.), *The Geology of South Africa*. Geological Society of South Africa/Council for Geoscience, Johannesburg/Pretoria, pp. 9–56.
- Buchan, K.L., Mertanen, S., Park, R.G., Pesonen, L.J., Elming, S.-A., Abrahamsen, N., Bylund, G., 2000. Comparing the drift of Laurentia and Baltica in the Proterozoic: the importance of key palaeomagnetic poles. *Tectonophysics* 319 (3), 167–198.
- Cañón-Tapia, E., 1994. AMS parameters: guidelines for their rational selection. *Pure and Applied Geophysics* 142, 365–382.
- Cawthorn, R.G., Eales, H.V., Walraven, F., Uken, R., Watkeys, M.K., 2006. The Bushveld complex. In: Johnson, M.R., Anhaeusser, C.R., Thomas, R.J. (Eds.), *The Geology of South Africa*. Geological Society of South Africa/Council for Geoscience, Johannesburg/Pretoria, pp. 261–281.
- Chadima, M., Gunther, A., Hirt, A.M., Hrouda, F., Siemes, H., 2004. Phyllosilicate preferred orientation as a control of magnetic fabric: evidence from neutron texture goniometry and low and high-field magnetic anisotropy (SE Rhenohercynian Zone of Bohemian Massif). In: Martin-Hernandez, F., Luneburg, C.M., Aubourg, C., Jackson, M. (Eds.), *Magnetic Fabric: Methods and Applications*. Geological Society, London, pp. 361–380 (Special Publications, 238).
- Cheney, E.S., 1996. Sequence stratigraphy and plate tectonic significance of the Transvaal succession of southern Africa and its equivalent in Western Australia. *Precambrian Research* 79, 3–24.

- de Kock, M.O., Evans, D.A.D., Kirschvink, J.L., Beukes, N.J., Rose, E., Hilburn, I., 2009. Paleomagnetism of a Neoproterozoic–Paleoproterozoic carbonate ramp and carbonate platform succession (Transvaal Supergroup) from surface outcrop and drill core, Griqualand West region, South Africa. *Precambrian Research* 169 (1–4), 80–99.
- Duncan, A.R., Marsh, J.S., 2006. The Karoo igneous province. In: Johnson, M.R., Anhaeusser, C.R., Thomas, R.J. (Eds.), *The Geology of South Africa. Geological Society of South Africa/Council for Geoscience, Johannesburg/Pretoria*, pp. 501–520.
- Eglington, B.M., Armstrong, R.A., 2004. The Kaapvaal Craton and adjacent orogens, southern Africa: a geochronological database and overview of the geological development of the craton. *South African Journal of Geology* 107, 13–32.
- Elming, S.-Å., Mattsson, H., 2001. Post Jotnian basic intrusion in the Fennoscandian Shield, and the break up of Baltica from Laurentia: a palaeomagnetic and AMS study. *Precambrian Research* 108, 215–236.
- Enkin, R.J., 1994. A Computer Program Package for Analysis and Presentation of Paleomagnetic Data. Pacific Geoscience Center, Geological Survey of Canada, p. 16.
- Eriksson, P.G., Altermann, W., Hartzler, F.J., 2006. The Transvaal Supergroup and its precursors. In: Johnson, M.R., Anhaeusser, C.R., Thomas, R.J. (Eds.), *The Geology of South Africa. Geological Society of South Africa/Council for Geoscience, Johannesburg/Pretoria*, p. 691.
- Eriksson, P.G., Banerjee, S., Nelson, D.R., Rigby, M.J., Catuneanu, O., Sarkar, S., Roberts, R.J., Ruban, D., Mtimkulu, N.M., Ranu, P.V.S., 2009. A Kaapvaal craton debate: nucleus of an early small supercontinent or affected and enhanced by accretion event? *Gondwana Research* 15 (3–4), 354–372.
- Ernst, R.E., Baragar, W.R.A., 1992. Evidence from magnetic fabric for the flow pattern of magma in the Mackenzie giant radiating dyke swarm. *Nature* 356, 511–513.
- Evans, D.A., Beukes, N.J., Kirschvink, J.L., 1997. Low-latitude glaciation in the Palaeoproterozoic era. *Nature* 386, 262–266.
- Evans, D.A.D., Beukes, N.J., Kirschvink, J.L., 2002. Paleomagnetism of a lateritic paleoweathering horizon and overlying Paleoproterozoic red beds from South Africa: implications for the Kaapvaal apparent polar wander path and a confirmation of atmospheric oxygen enrichment. *Journal of Geophysical Research*, 107, doi:10.1029/2001JB000432 (No. BN12, 2326).
- Fisher, R., 1953. Dispersion of sphere. *Proceedings of the Royal Society, London A* 217, 293–305.
- Gold, D.J.C., 2006. The Pongola Supergroup. In: Johnson, M.R., Anhaeusser, C.R., Thomas, R.J. (Eds.), *The Geology of South Africa. Geological Society of South Africa/Council for Geoscience, Johannesburg/Pretoria*, pp. 135–147.
- Hanson, R.E., Gose, W.A., Crowley, J.L., Ramezani, J., Bowring, S.A., Bullen, D.S., Hall, R.P., Pancake, J.A., Mukwakeami, J., 2004. Paleoproterozoic intraplate magmatism and basin development on the Kaapvaal Craton: age, paleomagnetism and geochemistry of ~1.93 to ~1.87 Ga post-Waterberg dolerites. *South African Journal of Geology* 107, 233–254.
- Hargraves, R.B., Rehacek, J., Hooper, P.R., 1997. Palaeomagnetism of the Karoo igneous rocks in southern Africa. *South African Journal of Geology* 100 (2), 195–212.
- Hattingh, P.J., 1986. The paleomagnetism of the Merensky Reef footwall rocks of the Bushveld Complex. *Transactions of the Geological Society of South Africa* 89, 1–8.
- Hrouda, F., 1982. Magnetic anisotropy of rocks and its application in geology and geophysics. *Survey of Geophysics* 5, 37–82.
- Hunter, D.R., Halls, H.C., 1992. A geochemical study of a Precambrian mafic dyke swarm, Eastern Transvaal, South Africa. *Journal of African Earth Sciences* 15, 153–168.
- Hunter, D.R., Johnson, M.R., Anhaeusser, C.R., Thomas, R.J., 2006. Geology of the South Africa. Introduction. *The Geological Society of South Africa*, 1–9.
- Jacobs, J., Pisarevsky, S., Thomas, R.J., Becker, T., 2008. The Kalahari Craton 952 during the assembly and dispersal of Rodinia. *Precambrian Research* 160, 142–158.
- Jelinek, V., 1981. Characterization of the magnetic fabric of rocks. *Tectonophysics* 79, 63–67.
- Johnson, M.R., Anhaeusser, C.R., Thomas, R.J., 2006. *The Geology of South Africa. Geological Society of South Africa. Johannesburg/Council for Geoscience, Pretoria*, 691 p.
- Jourdan, F., Feraud, G., Bertrand, H., Watkeys, M.K., Kampunzu, A.B., Le Gall, B., 2006. Basement control on dyke distribution in Large Igneous Provinces: case study of the Karoo triple junction. *Earth and Planetary Sciences Letters* 241, 307–322.
- Klausen, M.B., 2009. The Lebombo monocline and associated feeder dyke swarm: diagnostic of a successful and highly volcanic rifted margin? *Tectonophysics* 468, 42–62.
- Klausen, M.B., Söderlund, U., Olsson, J.R., Ernst, R.E., Armoogam, M., Mkhize, S.W., Petzer, G., 2010. Petrological discrimination among Precambrian dyke swarms, Eastern Kaapvaal Craton (South Africa). *Precambrian Research* 183, 501–522.
- Knight, M.D., Walker, G.P.L., 1988. Magma flow directions in dikes of the Koolau Complex, Oahu, determined from magnetic fabric studies. *Journal of Geophysical Research* 93, 4301–4319.
- Kirschvink, J.L., 1980. The least-squares line and plane and the analysis of paleomagnetic data. *Geophysical Journal of the Royal Astronomical Society* 62, 699–718.
- Layer, P.W., 1986. Archean paleomagnetism of southern Africa. Ph.D. Thesis. Stanford University, p. 397.
- Layer, P.W., Kröner, A., McWilliams, M., 1988. Paleomagnetism and the age of the Archean Usushwana Complex, Southern Africa. *JGR* 93B1, 449–457.
- Layer, P.W., Kröner, A., McWilliams, M., York, D., 1989. Elements of Archean thermal history and apparent polar wander of the eastern Kaapvaal Craton, Swaziland, from single grain dating and paleomagnetism. *Earth and Planetary Sciences Letters* 93, 23–34.
- Layer, P.W., Lopez-Martinez, M., Kröner, A., York, D., McWilliams, M., 1998. Thermochronometry and palaeomagnetism of the Archean Nelshoogte Pluton, South Africa. *Geophys. J. Int.* 135, 129–145.
- Mapeo, R.B.M., Ramokate, L.V., Corfu, F., Davis, D.W., Kampunzu, A.B., 2006. The Okwa basement complex, western Botswana: U–Pb zircon geochronology and implications for Eburnean processes in southern Africa. *Journal of African Earth Sciences* 46, 253–262.
- McFadden, P.L., McElhinny, M.W., 1990. Classification of the reversal test in paleomagnetism. *Geophysical Journal International* 103, 725–729.
- Nelson, D.R., Trendall, A.F., Altermann, W., 1999. Chronological correlations between the Pilbara and Kaapvaal cratons. *Precambrian Research* 97, 165–189.
- Olsson, J.R., Söderlund, U., Klausen, M.B., Ernst, R.E., 2010. U–Pb baddeleyite ages of major Archean dyke swarms and the Bushveld Complex, Kaapvaal Craton (South Africa): correlations to volcanic rift forming events. *Precambrian Research* 183, 490–500.
- Palmer, H.C., Ernst, R.E., Buchan, K.L., 2007. Magnetic fabric studies of the Nipissing sill province and Senneterre dykes, Canadian Shield, and implications for emplacement. *Canadian Journal of Earth Sciences* 44, 507–528.
- Park, J.K., Tanczyk, E.I., Desbarats, A., 1988. Magnetic fabric and its significance in the 1400 Ma Mealy diabase dykes of Labrador, Canada. *Journal of Geophysical Research* 93, 13689–13704.
- Pisarevsky, S.A., 2005. New edition of the Global Paleomagnetic Database. *EOS transactions* 86 (17), 170.
- Polteau, S., Ferré, E.C., Planke, S., Neumann, E.-R., Chevallier, L., 2008. How are saucer-shaped sills emplaced? Constraints from the Golden Valley sill, South Africa. *Journal of Geophysical Research* 113, B12104, doi:10.1029/2008JB005620.
- Potter, D.K., Stephenson, A., 1988. Single-domain particles in rocks and magnetic fabric analysis. *Geophysical Research Letters* 15, 1097–1100.
- Reeves, C., 2000. The geophysical mapping of Mesozoic dyke swarms in southern Africa and their origin in the disruption of Gondwana. *Journal of African Earth Sciences* 30, 499–513.
- Robb, L.J., Brandl, G., Anhaeusser, C.R., Poujol, M., 2006. Archean granitoid intrusions. In: Johnson, M.R., Anhaeusser, C.R., Thomas, R.J. (Eds.), *The Geology of South Africa. Geological Society of South Africa/Council for Geoscience, Johannesburg/Pretoria*, pp. 57–94.
- Rochette, P., Aubourg, C., Perrin, M., 1999. Is this magnetic fabric normal? A review and case studies in volcanic formations. *Tectonophysics* 307, 219–234.
- Rogers, J.J.W., 1996. A history of continents in the past three billion years. *The Journal of Geology* 104, 91–107.
- Söderlund, U., Hofmann, A., Klausen, M.B., Olsson, J.R., Ernst, R.E., 2010. Towards a complete magmatic barcode for the Zimbabwe craton: baddeleyite U–Pb dating of regional dolerite dike swarms and sill provinces. *Precambrian Research* 183, 388–398.
- Strik, G., de Wit, M.J., Langereis, C.G., 2007. Palaeomagnetism of the Neoproterozoic Pongola and Ventersdorp Supergroups and an appraisal of the 3.0–1.9 Ga apparent polar wander path of the Kaapvaal Craton, Southern Africa. *Precambrian Research* 153, 96–115.
- Tarling, D.H., Hrouda, F., 1993. *The Magnetic Anisotropy of Rocks*. Chapman & Hall, London, p. 217.
- Uken, R., Watkeys, M.K., 1997. An interpretation of mafic dyke swarms and their relationship with major mafic magmatic events on the Kaapvaal Craton and Limpopo Belt. *South African Journal of Geology* 100, 341–348.
- Walraven, F. and Hartzler, F.J., 1986. Sheet 2530 Barberton (1:250 000 Geological Series). *Geol. Surv. S. Afr.*
- Watson, G.S., 1956. A test for randomness of distributions. *Mon. Not. Roy. Astron. Soc. Geophys.* 7, 160–161.
- Wingate, M.T.D., 1998. A palaeomagnetic test of the Kaapvaal–Pilbara (Vaalbara) connection at 2.78 Ga. *South African Journal of Geology* 101 (4), 257–274.
- Zijderveld, J.D.A., 1967. Demagnetization of rocks: analysis of results. In: Collinson, D.V., Creer, K.M., Runcorn, S.K. (Eds.), *Methods in Palaeomagnetism*. Elsevier, New York, pp. 254–286.